VOL. 10 No. 8, pp. 221-256 FEBRUARY 1949

Philips Technical Review

DEALING WITH TECHNICAL PROBLEMS
RELATING TO THE PRODUCTS, PROCESSES AND INVESTIGATIONS OF
THE PHILIPS INDUSTRIES

EDITED BY THE RESEARCH LABORATORY OF N.V. PHILIPS' GLOEILAMPENFABRIEKEN, EINDHOVEN, NETHERLANDS

A MINIATURE X-RAY APPARATUS FOR DENTISTS

by J. FRANSEN.

616.314-073.75

For taking intra-oral radiographs of the teeth and mandible only a small X-ray intensity is needed. An apparatus for this purpose, therefore, need only be of small power (e.g. 160 W) with a relatively low tube voltage (45 kV$_{\text{peak}}$). Moreover the voltage and current do not have to be variable. These simplifications have made it possible to construct for dental use an X-ray apparatus of extremely small dimensions and light weight (4.5 kg). The X-ray tube, built on the lines of a modern radio valve, is only 6 cm ($2^3/_8$″) long. The X-ray tube and the high tension transformer are contained in a shield filled with oil. The filament current is drawn from a winding on the high tension transformer. The tube current is nevertheless sufficiently insensitive to mains voltage fluctuations, the cathode being made to work in the space-charge range instead of the saturation range. The circuit used for this purpose also has an additional stabilizing action. This article deals with all these points and describes the construction of the transformer as well as the apparatus as a whole.

The making of X-ray photos of the human denture and the designing of an apparatus for that purpose are in every respect much simpler problems than those usually encountered in medical X-ray practice, the most important differences being the following:

1) The object to be photographed does not make any involuntary movements like those of the lungs, heart and stomach, so that from the point of view of sharpness of definition a longer exposure time can be allowed.
2) The part of the body to be X-rayed (the mandible) is at most 2-2.5 cm thick, so that the focus of the X-ray tube can be brought close to the object (and thus to the film) without any troublesome distortion in the shadow picture. Since all parts of the object are close to the film, there is also little geometrical blurring of any parts.
3) Thanks to the nature and thinness of the object, relatively little radiation is absorbed. Due to the closeness of the focus to the film and the possibility of long exposure with a reasonably sensitive film, there is no need for an intensive radiation for radiography [1]). The advantages thus offered are:
   a) A relatively small-power X-ray tube suffices.
   b) Particularly, a low tube voltage can be chosen. This is not only an advantage from the constructional point of view but with such thin objects it is even an essential condition in order to get proper contrasts in the picture.
   c) The small power required can be dissipated on a relatively small focus, thus enhancing the definition of the radiograph.
4) In intra-oral radiography there are very little differences in the thickness and composition of the layers of tissue that have to be penetrated, so that there is no need for the tube voltage and the current to be made variable; small differences in absorption can easily be compensated by varying the exposure time if the same average film blackening is required.
5) Corresponding to the smallness of the objects, is a small size film. There is therefore no need, from the point of view of expense, for screening instead of radiographing. As a matter of fact there is an objection against screening, because

---

[1]) There is, it is true, also a factor having the opposite effect. Owing to the relatively high demands made in respect to the sharpnesss of dental photographs, no intensifying screens are applied to the film, because these would cause considerable blurring due to their granular structure. This means that the intensity has to be about 10 times as great as that needed when intensifying screens are used. Still the gain in intensity obtained by the aforementioned factors is by far the greater.

of the considerable screen-blurring and the large X-ray dose that would have to be given to the patient. The X-ray apparatus need not, therefore, bear any considerable loads.

The fact that the requirements to be met in the design of a dental X-ray apparatus can easily be satisfied does not by any means imply that the product is technically less interesting. As a matter of fact these simple conditions made it possible to improve considerably upon other diagnostic apparatus of a higher capacity, as far as small dimensions, simple construction and handiness are concerned. In *table I* some data of a new apparatus ("Oralix") specially designed by Philips for dentists are compared with those of a universal diagnostic apparatus ("Medio D" [2])). *Fig. 1* is a photograph showing the apparatus mounted on a dental chair.

The description that will now be given of this

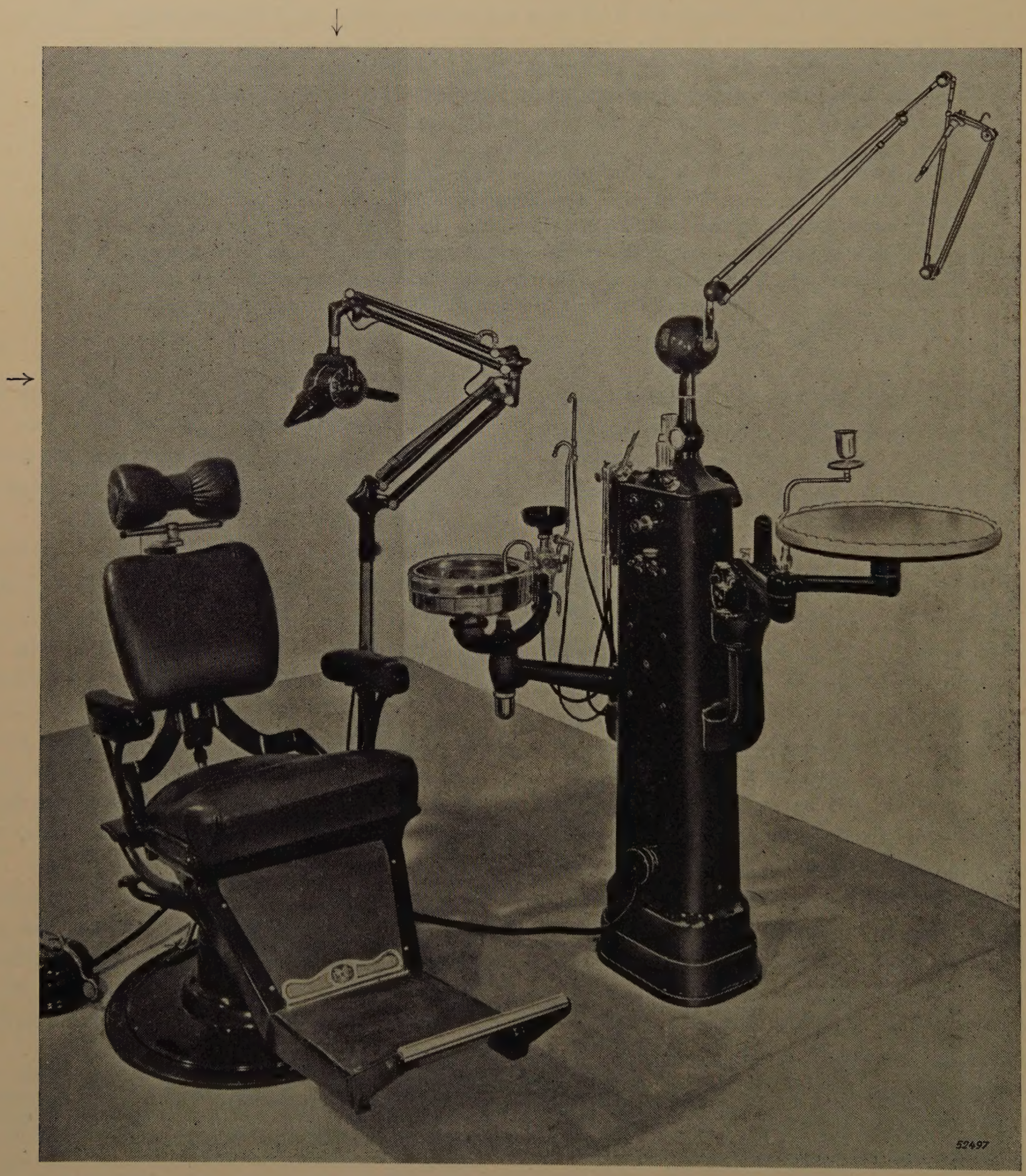

Fig. 1. The "Oralix" miniature X-ray unit developed by Philips. The aparatus (see directions of the arrows) is shown on an arm attached to a dental chair.

---

[2]) H. A. G. Hazeu and J. M. Ledeboer. A universal apparatus for X-ray diagnosis, Philips Techn. Rev. **6**, 12-20, 1941. A dental apparatus built on principles similar to those described here and weighing even less was demonstrated by Bouwers already in 1937 at the fifth international roentgenological congress at Chicago (see A. Bouwers and W. J. Oosterkamp, Amer. J. Radium Therapy, **41**, 444-447, 1938), but owing to manufacturing problems this apparatus was not produced in any large numbers.

Table I. Comparison between some data of a universal diagnostic apparatus ("Medio D") and those of the new dental X-ray apparatus ("Oralix").

	"Medio D"	"Oralix"
Tube voltage	45-100 $\mathrm{kV_{peak}}$	45 $\mathrm{kV_{peak}}$
Tube current for radiography	100-250 mA	5 mA
Tube current for screening	3 mA	—
Time range	0.02-8.0 sec	0.1-6.0 sec
Focus width	1.2 or 2.0 or 3.5 mm	0.8 mm
Load-capacity, intermittent	13 kW	160 W
Load-capacity, continuous	150 W	(16 W)
Weight of X-ray tube	20 kg	4.5 kg
Weight of generator	300 kg	
Length of X-ray tube	30 cm	6 cm

miniature apparatus will show how the utmost advantage has been taken of the aforementioned possibilities for a small and simple construction.

The X-ray tube

The X-ray tube is made of hard glass and insulated in oil. As already described on more than one occasion [3]), this allows of a considerable reduction in the length of the insulation required for the tube voltage, and thus in the length of the tube. In our case, where a voltage of only 45 $\mathrm{kV_{peak}}$ was required, the minimum length of tube was in fact so small that the problem arose how to fit in the cathode and anode with their leads in such a way as to profit from this possibility of reducing dimensions.

The solution found is shown in *fig. 2*. Instead of the cathode being fused into the tube with the conventional pinch, as is done for larger X-ray tubes, the base of the tube is made flat and of hard glass, following the example of modern radio valves. Fused into the base are four molybdenum pins, which can act at the same time as connecting pins, leads, and as supports for the cathode system mounted in the tube. The solid tungsten anode is attached to a molybdenum pin carried through the top of the tube by the usual fusing technique. The resultant small dimensions are illustrated in fig. 2.

The filament is placed in a cathode cap which ensures focusing of the emitted electrons upon the small area of 0.8 mm × 3 mm on the anode (line focus, which in oblique projection has the apparent dimensions of 0.8 mm × 0.8 mm).

The thin anode pin cannot contribute much to carrying off the heat generated on the focus from the anode outwards. The anode therefore has to dissipate this heat for the greater part by radiation.

The following calculation shows that the anode is indeed able to do this. The heat developed during an exposure time of 6 seconds (the maximum exposure time this apparatus permits) is equivalent to 950 Wsec for an A.C. voltage of 45 $\mathrm{kV_{peak}}$ and 5 mA average tube current. The mass of the anode being 66 grams, the heat capacity is 9.4 Wsec/°C. The rise in temperature while making one radiograph is thus roughly 100 °C. Since at the most one has to reckon with intermittent working with one exposure of such a length per minute, the anode cannot cool off to room temperature after each photograph is taken, so that a certain higher starting temperature has to be reckoned with. While a photograph is being taken the anode temperature must not be allowed to rise above 850 °C, so that the starting temperature may be 750 °C at the utmost. Thus the anode has to cool off each time from 850 to 750 °C within one minute and by radiation. Now the formula for the total radiation of a black body of temperature T_1 °K is:

$$P = \delta \cdot (T_1^4 - T_0^4)\ \mathrm{W/cm^2},$$

where $\delta = 5.8 \times 10^{-12}$ W/cm² degree and T_0 is the ambient temperature. The radiation of polished tungsten is much less, at 1100 °K for instance being equal to that of a black body at a temperature of 659 °K. In the case of our anode we can take it that radiation takes place at an average temperature between 1023 and 1123 °K, thus equal to that of a black body of about 640 °K. From the formula above we find that the radiation is $P = 0.92$ W/cm². The surface area of the anode being 13 cm², it radiates about 700 W sec/min, whilst 950 Wsec is added.

The excess of about 250 Wsec is carried off via the anode pin by conduction.

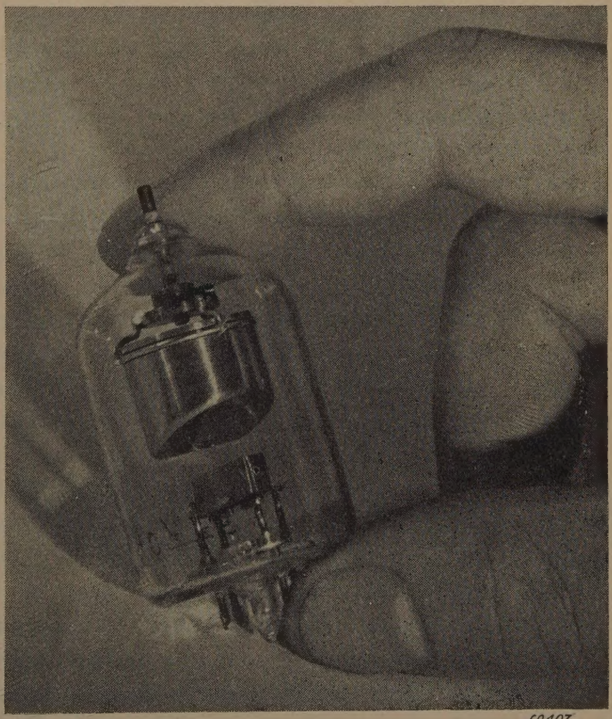

Fig. 2. X-ray tube for the "Oralix" miniature X-ray apparatus. The tube is designed to work on A.C. with 45 kV peak and 5 mA (mean) for max. 6 seconds per minute.

---

[3]) See, for instance, J. H. van der Tuuk, Hard glass X-ray tubes in oil, Philips Techn. Rev. 6, 309-315, 1941.

The heat irradiated is first absorbed by the oil surrounding the tube and then imparted to the shield. In addition to its insulating effect the oil therefore has a cooling function.

The supply and stabilization of the tube current

A diagram of the circuit for feeding the X-ray tube is given in *fig. 3*. The secondary voltage from the high-tension transformer is conducted direct to the X-ray tube. The voltage for the filament is taken from a separate winding mounted on the secondary winding. Tube voltage and filament voltage are therefore in a fixed ratio. This simple method is possible in our case because neither the tube voltage nor the tube current need be varied, these being adjusted to the fixed values of 45 kV_{peak} and 5 mA (average value) respectively.

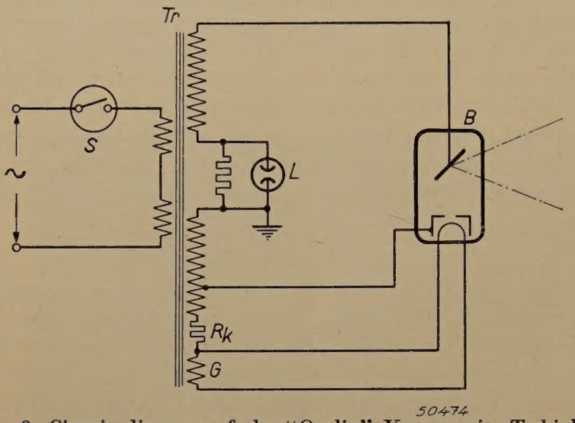

Fig. 3. Circuit diagram of the "Oralix" X-ray unit. *Tr* high tension transformer with symmetrical voltage with respect to earth; *B* X-ray tube; *G* heating-current winding; R_k resistor for applying a negative "grid bias" to the tube so that the filament works in the space-charge range of the characteristic curve; *L* pilot lamp; *S* time switch.

In normal X-ray apparatus where the tube current has to be variable the filament voltage is supplied by a separate small transformer; it can then be adjusted independently of the tube voltage, by adjusting the primary voltage on that transformer which is at a low potential. For a sensitive adjustment of the tube current the tube is caused to work in the saturation range of cathode emission; in fact, the saturation value of the cathode emission depends very strongly upon the cathode temperature. In this way a 50 % variation in the tube current is possible with a variation of only 10% in the filament voltage.

In our case, where only one fixed value of the tube current is required, working in the saturation range of the cathode is not only unnecessary but even undesirable, because otherwise the tube current would be highly sensitive to small fluctuations in the mains voltage. Since such a fluctuation generally passes unnoticed — in non-adjustable apparatus the voltage is not usually checked — and hence the current variation cannot be compensated by changing the exposure time, the film blackening would not be reproducible to the desired extent.

For this reason in our case the X-ray tube must not be allowed to work in the saturation range but rather in the space-charge range of the cathode emission.

In order to bring this about, one could try to reduce the action of the anode on the cathode through the opening of the cathode cap. This action, which can be defined as the reciprocal value of the amplification factor, will be denominated as the "transudation" (in foreign literature the common term is "Durchgriff"). A reduction of this "transudation" involves changing the configuration of the electrodes, for instance making the cathode cap narrower or placing the filament farther down in the cap. Such a method, however, would defeat its own object because, although the tube current is then much less sensitive to fluctuations in the filament voltage, the possibility is lost of obtaining the nominal value of tube current by adjusting the filament voltage in the manufacture. As a result one would be limited to extremely narrow tolerances in the electrode arrangement to obtain the nominal tube current without further adjustment.

Another course has therefore been chosen. The cathode cap, which in normal X-ray tubes is always at the potential of the filament, has been given a separate lead through the tube base. A voltage is now applied to the cap which is negative with respect to the filament. This "grid voltage" (v_g) is taken from a resistor (R_k) in the circuit through which the tube current flows; see fig. 3.

A diagram, as given in *fig. 4*, of the i_a-v_g characteristics of the X-ray tube — which can here be dealt with in a manner similar to that applied to a triode in the radio technique — shows that by this means the tube is indeed made to operate in the space-charge range. Each characteristic refers to a certain value of the anode voltage, the three fully-drawn curves relating especially to the peak values of the anode voltage in respect of the nominal, the maximum and the minimum mains voltages occurring ($V_{n\,\mathrm{nom}}$, $V_{n\,\max}$ and $V_{n\,\min}$ respectively). At any moment the grid voltage is

$$v_g = -R_k \cdot i_a \quad . \; . \; . \; . \; . \; . \; . \quad (1)$$

In each mains cycle the working point of the tube, which has the co-ordinates v_g and i_a, travels to and fro along the straight line given by eq. (1) and drawn through the origin — the working line —

thereby intersecting the family of characteristics according to the momentary values of the anode voltage passing through. The point where the working line intersects the curve $V_{n\,\mathrm{nom}}$ gives the peak value $I_{a\,\mathrm{nom}}$ of the tube current (in our case about 15 mA, corresponding to the previously mentioned mean value of 5 mA). It is seen that the working point is always within the sloping part of the curves (the space-charge zone), where they deviate much less than in the saturation zone.

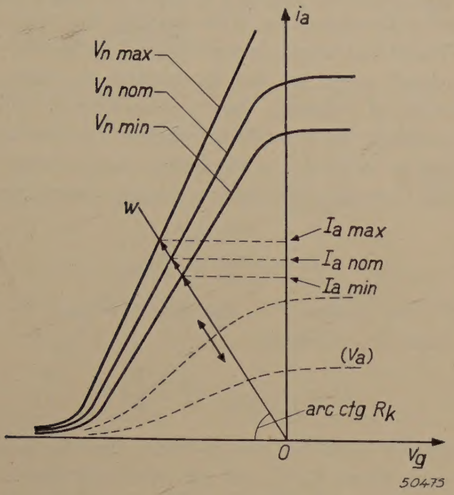

Fig. 4. Diagram of the i_a-v_g characteristics for the X-ray tube. Owing to the condition $v_g = -R_k i_a$, the working point has to move along the line w drawn through the origin. Each curve corresponds to a certain anode voltage. During a cycle of the alternating voltage supply the family of curves is intersected along the working line. The characteristic for the anode peak voltage occurring at the nominal value $V_{n\,\mathrm{nom}}$ of the mains voltage produces the peak value $I_{a\,\mathrm{nom}}$ of the tube current. With fluctuating mains voltage (between $V_{n\,\mathrm{max}}$ and $V_{n\,\mathrm{min}}$) there is relatively little variation in the tube current, owing to the characteristics deviating but little in the sloping part (space-charge range). Since with fluctuating mains voltage V_n the heating temperature of the cathode will fluctuate as well, the dotted curves for the instantaneous values v_a of the anode voltage will also vary slightly each time; for the sake of simplicity this is not shown here.

This method avoids the difficulty of too small tolerances in the electrode configuration. Fig. 4 shows that owing to the oblique traject of the working line the tube current I_a is less affected by small deviations in the characteristic, regardless whether these deviations are caused by variation of the mains voltage (thus of the filament voltage) or of the electrode configuration. Consequently, when a tube is being inserted in the apparatus there is no need to pay attention to the unavoidable small differences that exist between various tubes; the desired nominal tube current is obtained with sufficient accuracy without any adjustments.

To complete the picture *fig. 5* gives the corresponding diagram for the case where the X-ray tube is worked in the normal manner, thus with $R_k = 0$, in the saturation zone. Here the working line is the ordinate axis ($v_g = 0$) and it is seen that for the peak values of the anode voltage the working point enters the saturation range of the curves, resulting in the great differences between $I_{a\,\mathrm{max}}$ and $I_{a\,\mathrm{min}}$.

A comparison of the families of curves given in figs 4 and 5 shows that in fig. 4 the saturation values are much higher. This is necessary to bring the point of intersection of the working line on the characteristic for $V_{n\,\mathrm{nom}}$ on the same level as in fig. 5, thus to obtain the desired nominal tube current $I_{a\,\mathrm{nom}}$. The higher saturation is obtained by increasing the emission of the filament, for instance by heating it to a higher temperature.

In the foregoing we have dealt with the i_a-v_g diagram of our X-ray tube in a manner similar to that applied for a radio valve. Actually, however, there is an important difference, also in the qualitative sense. In the case of a radio valve the filament voltage is usually kept constant, so that in the i_a-v_g diagram of such a valve the characteristics corresponding to different anode voltages (V_a) all have the same slope. Where we have a working line like that in fig. 4 the relative variation of the tube current I_a corresponding to a variation in the anode voltage is always equal to the relative variation of V_a. In the case of our X-ray tube, however, the filament voltage also varies together with the anode voltage. Consequently the curves become steeper as V_a increases and the beam diverges, resulting in a relatively stronger variation of I_a.

It now appears that circuiting with the resistor R_k has another particular advantage compared with the other method of bringing the working point within the space-charge range (reducing the "transudation"). With the latter method, where $R_k = 0$, the working line of the diagram is the ordinate axis ($v_g = 0$), so that the diverging family of characteristics is intersected in the

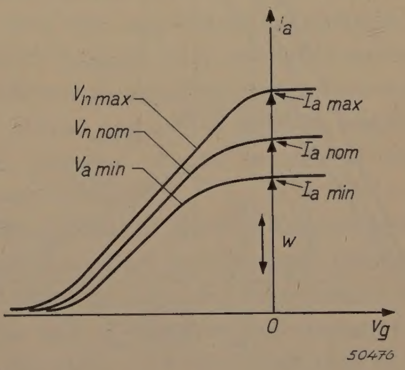

Fig. 5. Diagram corresponding to that in Fig. 4, for the case where the X-ray tube operates in the normal manner, with the filament working in the saturation range. Here the working line w is the ordinate axis ($v_g = 0$). The variations of I_a accompanying fluctuations in the mains voltage V_n are very considerable.

vertical direction [4]). As a result any variation in V_a causes about twice as large a variation in I_a. In Fig. 4 on the other hand, where $R_k > 0$, the characteristics are intersected obliquely, so that their divergence is much less felt and I_a varies for instance by a factor of only $1^1/_2$ with respect to V_a.

Obviously this additional stabilizing action — just like the effect of rendering the tube current insensitive to the tolerances in the electrode configuration — will be all the more successful the larger the resistor R_k is chosen, for the working line in fig. 4 will then be flatter. But then, unless other steps are raken, the point of intersection of the working line on the characteristic $V_{n\,\mathrm{nom}}$ will be lower. Now, to be able to choose a large value of R_k and still reach the prescribed value of $I_{a\mathrm{nom}}$ for the tube current with the given characteristic, a positive grid bias has, in addition, been applied. This is obtained by connecting the cathode cap to a tapping of the high tension transformer as indicated in fig. 3 instead of connecting it direct to R_k. The resultant grid voltage is then at any moment

$$v_g = fv_a - i_aR_k, \quad \ldots \ldots \quad (2)$$

where f denotes the fraction of the high-tension coil to which the tapping is made. The working point for any moment can be found from the dotted line construction in *fig. 6*. Inversely, by starting from given values for $I_{a\,\mathrm{nom}}$ and R_k, with this construction it is possible to determine the required value of $f\,V_{a\,\mathrm{nom}}$ and thus of f.

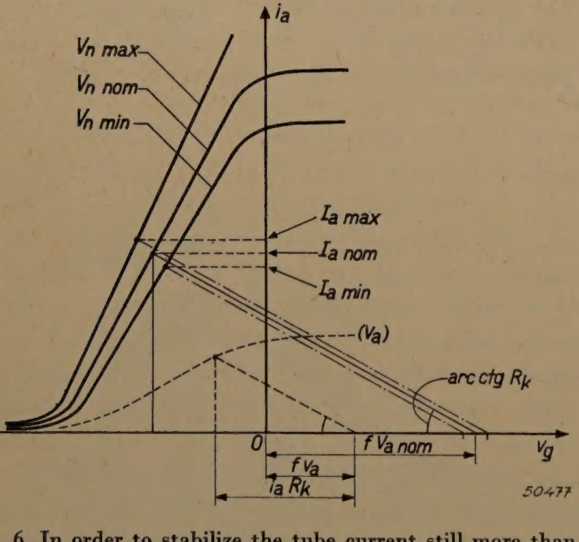

Fig. 6. In order to stabilize the tube current still more than in fig. 4 the resistor R_k has been made larger, and in order to obtain the same value for $I_{a\,\mathrm{nom}}$ a positive grid voltage component fv_a has been added. The resultant grid voltage v_g is at any moment the difference between fv_a and i_aR_k. The dotted lines indicate how the position of the working point is found at any moment (v_a, thus fv_a, and R_k given). The $I_{a\,\mathrm{nom}}$ and (dot-dash lines) $I_{a\,\mathrm{max}}$ and $I_{a\,\mathrm{min}}$ values can be constructed in the same way.

Since for the case of fig. 6 the working line cannot be indicated offhand, one cannot immediately visualize the "additional stabilization" given by the R_k method as compared with the method of reducing the "transudation". This can be found, however, by a simple calculation. For the X-ray tube, considered as a triode, in the space-charge range (the part where the characteristics show a straight slope) the equation holds:

$$i_a = S\left(v_g + \frac{v_a}{\mu}\right), \quad \ldots \ldots \ldots \quad (3)$$

where S is the slope and $1/\mu$ the "transudation". By substituting v_g from (2) we obtain

$$i_a = \frac{S}{1+SR_k}\cdot\left(f+\frac{1}{\mu}\right)v_a \quad \ldots \ldots \quad (4)$$

This equation holds for any moment, thus for instance also for the peak values I_a, V_a and the value of S corresponding to V_a. By taking the logarithms on both sides of the equation and differentiating we find

$$\frac{\mathrm{d}I_a}{I_a} = \frac{\mathrm{d}V_a}{V_a} + \frac{\mathrm{d}S}{S\,(1+SR_k)} \quad \ldots \ldots \quad (5)$$

This equation confirms in the first place the statement that in the most favourable case, i.e. when the slope S of the characteristics is independent of V_a, the relative tube current variation is not greater — but never less either — than the relative mains voltage variation. Actually we may take it that S is approximately proportional to the filament voltage, thus also proportional to V_a. For $R_k = 0$ it then immediately follows from (5) that $\mathrm{d}I_a/I_a = 2\mathrm{d}V_a/V_a$ (see above). We may furthermore write for our X-ray tube $S \approx 10^{-4}$ A/V. Hence

$$\text{for}\quad R_k = 0\ \text{ohm}: \quad \frac{\mathrm{d}I_a}{I_a} = 2\,\frac{\mathrm{d}V_a}{V_a},$$

$$R_k = 5000\ \text{ohms}: \quad = 1{,}7\,\frac{\mathrm{d}V_a}{V_a},$$

$$R_k = 10\,000\ \text{ohms}: \quad = 1{,}5\,\frac{\mathrm{d}V_a}{V_a},$$

$$R_k = 40\,000\ \text{ohms}: \quad = 1{,}2\,\frac{\mathrm{d}V_a}{V_a}.$$

By applying the indicated values of the resistance, the tube current variation for 10% mains voltage fluctuation is thus reduced to 20, 17, 15 and 12% respectively.

In practice a limit is set to the increasing of R_k by the fact that also the positive grid voltage contribution fv_a has to be chosen higher. In the half cycle when no tube current is flowing (v_a negative) the whole of the voltage fv_a (in this interval negative) comes to lie between the grid and the filament, and if this is too great it causes insulation troubles. Moreover, the effect of increasing R_k diminishes the higher the R_k values are chosen (see eq. (5)).

In the designing of the "Oralix" apparatus we have chosen R_k = 40 000 Ohms, at which value the tube current variation is only 1.2 times the mains voltage fluctuation causing that variation. The total gain obtained compared with the traditional circuiting of X-ray tubes where they work in the saturation range is shown graphically in *fig. 7*, where the tube current is plotted as function of the relative mains voltage.

---

[4] In order to obtain the same nominal tube current as indicated in fig. 4 the whole family of curves has to be imagined as being displaced to the right; this corresponds to a reduced transudation.

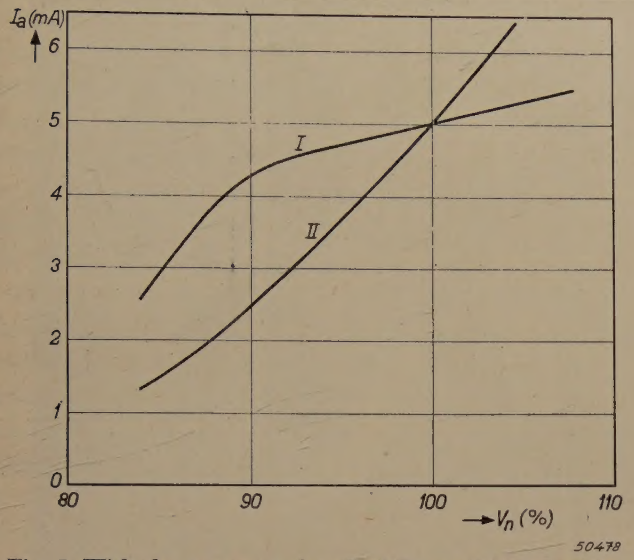

Fig. 7. With the apparatus described $R_k = 40\,000$ ohms has been chosen. Here the average tube current I_a is plotted as a function of the relative mains voltage V_n (% of the nominal value) and follows the curve *I*. If the X-ray tube were worked in the usual manner in the saturation range of the filament then the relation would be as represented by curve *II*.

As regards the film blackening, which is the criterion, it must not be forgotten that this is, of course, also affected by the tube voltage variation itself. Practice has shown that with $R_k = 40\,000$ ohms mains voltage fluctuations up to ± 5% can be allowed without any appreciable difference in the film blackening.

It is also to be pointed out that the negative grid bias on the cathode cap affects the shape of the potential field between filament and anode and therefore also the focusing effect of this field upon the electrons. Consequently this must be taken into account when deciding what shape is to be given to the electrodes. Since the total grid voltage does not vary proportionately with the tube voltage, variations in the mains voltage cause such a slight change in the size of the focus as to make this effect imperceptible in practice.

Construction of the high-tension transformer

The high-tension transformer and the X-ray tube are both mounted in a common shield. In order to derive full advantage from the small dimensions of the tube every attempt has been made to minimize also the transformer dimensions. The shell type of transformer has therefore been chosen, with the shell extended so as to envelop about five-sixths of the circumference of the coils. This construction, which had already been applied to a small X-ray apparatus previously described 5), has a very much smaller volume than the usual type. *Fig. 8* gives a clear picture of the construction. The iron circuit is made in two halves and after the coils, likewise made in two parts, have been fitted in, these two halves are placed face to face and tightly drawn together with bolts.

For easy shaping the shell is made by casting; the central part of the core is laminated and cast in the shell. To keep the eddy current losses in the non-laminated shell as low as possible the effect of the lamination is imitated by giving the shell the ribbed profile seen in fig. 8, whilst the material chosen is an iron alloy having a low electric conductivity. Nevertheless, with such a construction relatively large losses are unavoidable, but considering the small power of the apparatus such losses can be accepted from the economic point of view. We have therefore not hesitated to take advantage of this by allowing for a relatively heavy loading of the copper and the iron, thereby making it possible to reduce the dimensions and weight to the utmost. The losses only become objectionable when the heat thereby dissipated to the surroundings via the shield begins to obstruct the free dissipation of the "useful" heat generated on the anode (useful because this heat bears a fixed though very large ratio to the useful X-ray energy generated). This only occurs when the losses become about as great as the anode dissipation (160 W), a limit that is not reached with this apparatus. Incidentally, it was only possible to reach such small dimensions due to the oil dielectric in which the transformer and X-ray tube are placed and which greatly simplified the insulation problem (for a voltage of 25 $\mathrm{kV_{peak}}$ with respect earth.)

The copper losses of the high-tension transformer are in fact somewhat more limited than would be expected from the foregoing. They cause a voltage loss in the half cycle when the current is passing through the tube, with the result that in order to obtain a tube voltage of 45 $\mathrm{kV_{peak}}$ in this half cycle a higher no-load voltage is required, that is to say a higher voltage in the half cycle when there

---

5) A. Bouwers, Some new principles in design of X-ray apparatus, Radiology **22**, 163-173, 1934. See also H. A. G. Hazeu, Small apparatus for medical X-ray examination, Philips Techn. Rev. **6**, 225-234, 1941. The apparatus described there ("Centralix") worked with a higher voltage than the "Oralix", being designed for applications different from those occurring in dental practice.

is no load. Above a certain limit, therefore, the allowing of copper losses does more harm owing to the larger dimensions required to ensure sufficient insulation than the good derived from limiting the volume of copper. In our case the voltage drop is about 6 kV_{peak} for 5 mA (mean) tube current.

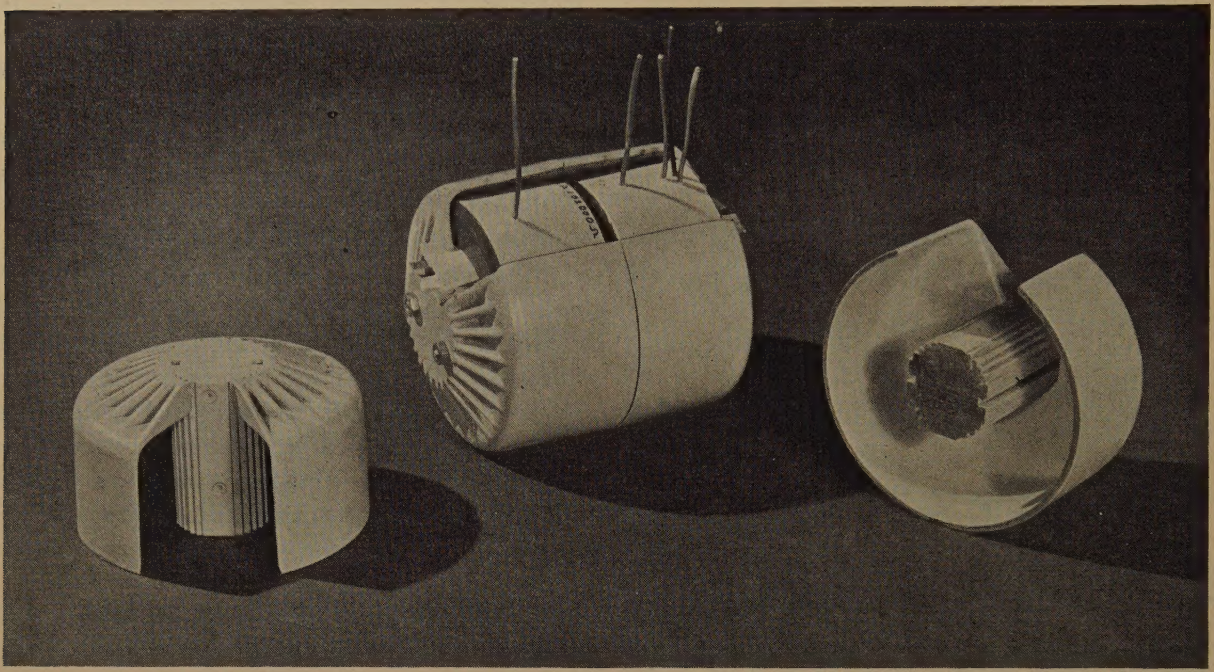

Fig. 8. In the middle, the high-tension transformer, completely assembled. On either side are the two halves of the iron circuit of a second specimen. Note the laminated central part and the cast shell extending over 5/6ths of the circumference.

Assembly of the apparatus

The manner in which the X-ray tube and the high-tension transformer are mounted in a common shield, likewise made in two halves, is shown clearly in *fig. 9*.

As already stated, the shield is filled with oil. The heat developed while the apparatus is working causes the oil to expand, whilst at lower temperatures, such as may prevail during transport, the volume of the oil is reduced. In order to ensure that these volume changes at temperatures between —10 and +60 °C do not cause any appreciable differences in pressure, an expansion vessel has been fitted into the shield in the form of a side tube shaped like an accordion.

The shield is made of brass. The X-rays emerge

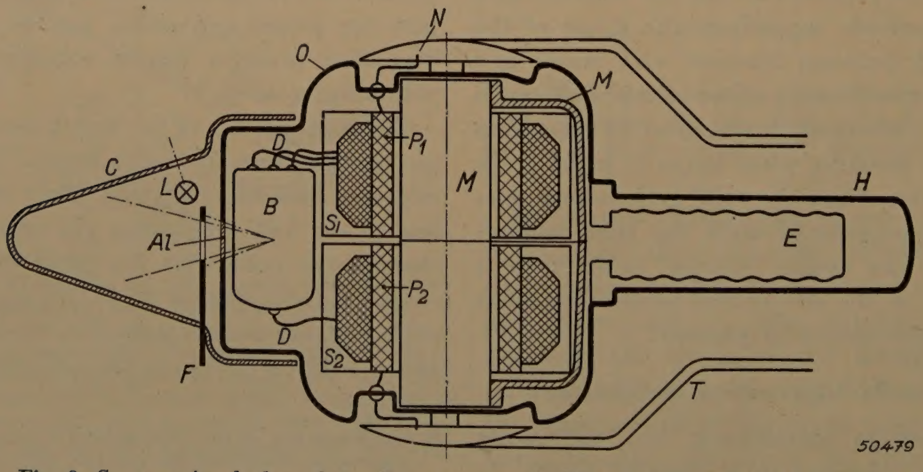

Fig. 9. Cross-sectional plan of the X-ray apparatus. *M* iron circuit of the high-tension transformer. P_1, P_2 halves of the primary coil, S_1, S_2 halves of the secondary winding, *D* connections to the X-ray tube *B*, *O* brass shield with aluminium window *Al*, *H* handle, *E* expansion vessel for the oil filling, *C* "Philite" directing cone, *T* bracket, *L* signal lamp, *F* exchangeable diaphragm, *N* mains lead.

through an aluminium window soldered in the brass wall. At this window the insulating layer of oil between the X-ray tube and the casing is only 3 mm thick. Owing to these measures the X-rays emitted are only slightly absorbed: the inherent filtration of the apparatus is equivalent to only 1 mm aluminium. This is of importance in connection with the fact that also the objects to be photographed absorb relatively little of the rays, about as much as 2 to 8 mm aluminium. On the other hand, the natural filter may not be much less than 1 mm aluminium because otherwise too many soft X-rays would be emitted, which, while not taking part in the image formation to any appreciable extent, might lead to an unnecessary amount of radiation being absorbed at the surface of the skin.

An exchangeable diaphragm can be placed in front of the window through which the X-rays emerge, thereby adapting the beam aperture to the size of the film, 2 × 3 or 3 × 4 or 4 × 5 cm. This adaptation is required because, if the beam is unnecessarily wide, the rays scattered in the object cause a loss in contrast in the X-ray picture [6]). If the same size of film is always used then as a rule there is no need to change the diaphragm, since the distance from focus to film is practically constant (about 12 cm). This distance is fixed on account of the fact that a directing cone of "Philite", the axis of which coincides with the axis of the X-ray beam, is mounted on the shield and pressed against the patient's face at the required spot (see fig. 11).

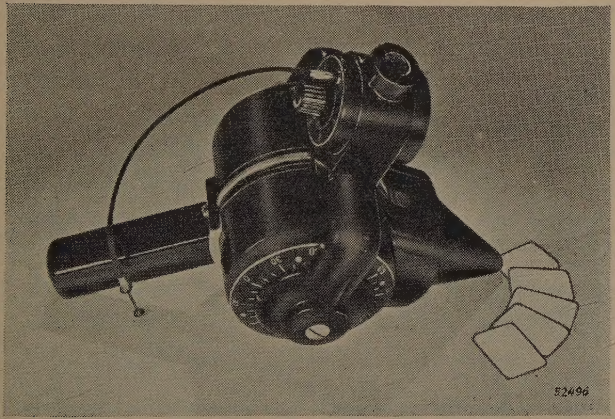

Fig. 10. Close-up of the miniature dental X-ray apparatus designed for suspension from a pulley (see fig. 11). Note the time switch on the trunnion. (In the design for mounting on a standard arm — see fig. 1 — the time switch is mounted in a separate hand switch.) The graduated scale is provided for adjusting the apparatus to the angle with respect to the "occlusal plane" required for radiographing each part of the denture. — Beside the apparatus are to be seen some dental films in their packing. Each packet contains two small films coated with emulsion on both sides; thus a duplicate is automatically made of each photograph. Behind the film in each packet is a tin foil protecting the films against fogging caused by the soft X-rays thrown back by the thumb of the patient when holding the film while the photograph is being taken.

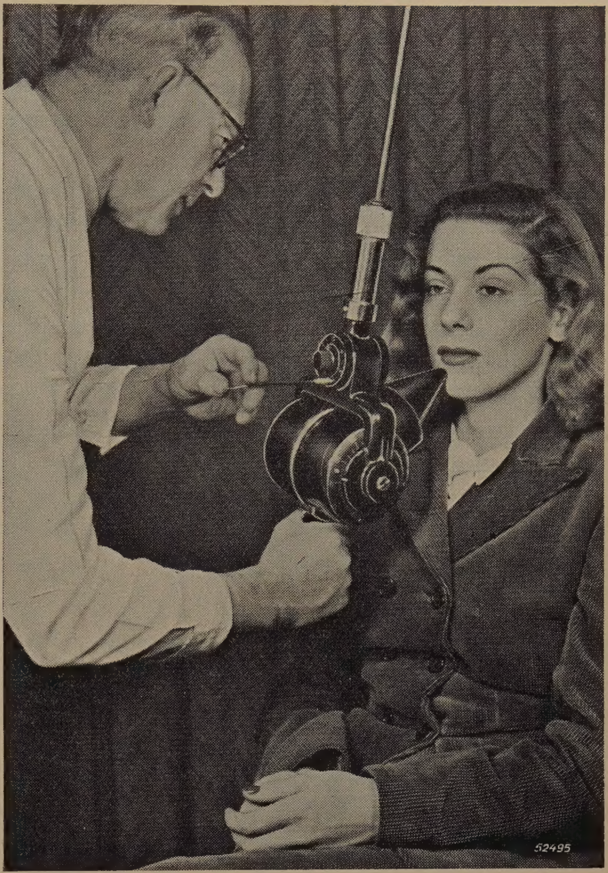

Fig. 11. The "Oralix" apparatus in use. The X-ray film is placed in the patient's mouth. (As a rule the patient has to press the film with the thumb against the part of the denture to be photographed.)

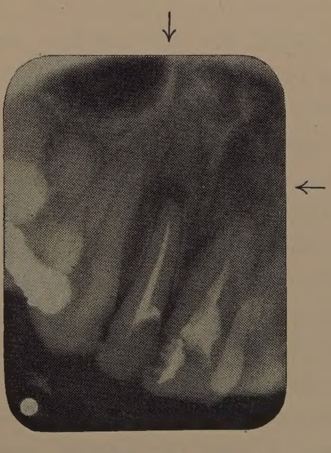

Fig. 12. Radiograph of part of an upper mandible taken with the "Oralix" apparatus, magnified 1.2 times. An inflammation is to be seen at the root of the second right-hand incisor (follow the arrows). The root channel is made clearly visible by a contrasting filling.

---

[6]) See, for instance, W. J. Oosterkamp, Eliminating scattered radiation in medical X-ray photographs, Philips Techn. Rev. **8**, 183-192, 1946, No. 6.

A small neon pilot lamp is fitted in the director cone and connected in the tube current circuit. When tube current is flowing this lamp lights up and can be seen through a slit during the course of the exposure.

Fig. 10 is a close-up photograph of the whole apparatus. The shield, which is rotatable around the horizontal axis, is held in a trunnion by means of which the apparatus can either be attached to an adjustable stand (see fig. 1) or suspended from the ceiling by means of a pulley wire (*fig. 11*). The bracket itself is rotatable round the vertical axis, so that the beam can be guided in any direction desired, for which purpose a handle has been provided on the shield. (The expansion tube referred to farther back is contained in this handle.) The mains lead is connected to the bracket, which (in the case of the pulley construction) also has a time switch for adjusting the exposure time (e.g. between $^1/_2$ and 3 seconds). This and the starting of the time switch by means of a wire relaxer are the only manipulations required for operating the apparatus, apart, of course, from aligning the film and the apparatus with the object to be photographed, and possibly a selection of diaphragm.

Finally in *fig. 12* a typical dental radiograph taken with the "Oralix" apparatus described is reproduced.

CERAMIC MATERIALS WITH A HIGH DIELECTRIC CONSTANT

by E. J. W. VERWEY and R. D. BÜGEL.

621.315.612.4:537.226.2

In electrical engineering, ceramic materials are very widely used for insulation purposes and as dielectric for capacitors. In the latter instance preference is given to a material having a high dielectric constant and low dielectric losses and here the choice is limited almost exclusively to pure titanium dioxide (rutile), or a mixture in which the latter figures as chief ingredient. Admixtures, sometimes necessary for the purpose of reducing the dielectric losses to a value below the permissible maximum, tend also to reduce considerably the dielectric constant of the TiO_2, and the purpose of this article is to investigate in how far the value of this constant is related to other properties of the material. A disadvantage of pure titanium dioxide is that the temperature coefficient of its dielectric constant is highly negative, The Philips Laboratories at Eindhoven have worked out various methods for reducing this temperature coefficient to zero by using suitable admixtures. By way of example, a description is given of a series of capacitors of small dimensions with a ceramic dielectric as used in radio receivers and other equipment incorporating high-frequency circuits.

Ceramic materials are widely employed for insulating purposes in electrical engineering: high values of the capacitance of the insulated conductors to earth, or in respect of other conductors, will, in general, involve a certain amount of hazard and such capacitances are therefore kept low by exercising care in the design and by employing a suitable ceramic material, i.e. one having a low dielectric constant.

The requirements imposed on insulating materials used as dielectric in capacitors are very different, however: here a high dielectric constant is usually an advantage, and certain ceramic materials can be produced which possess this property. Further, a suitable choice of the raw materials and methods of preparation will ensure that the resultant material meets certain other requirements to which capacitors usually have to conform, e.g. that the dielectric losses will not be too high and that the dielectric constant will not vary too much with the temperature.

Dielectric constant of titanium dioxide and the effects of admixtures

Those materials which have a high dielectric constant and which have so far been adopted for electrical purposes usually contain a major proportion of titanium dioxide, owing to the fact that this material (as also a number of titanates) belongs to the very small group of substances the dielectric constant of which is exceptionally high. In nature titanium dioxide (TiO_2) occurs in the form of three different modifications, namely anatase, brookite and rutile. Wherever titanium dioxide is mentioned in the following we mean rutile, this being the stable modification, having at the same time the greatest density as well as the highest index of refraction and dielectric constant.

The two last mentioned qualities are dependent, moreover, on the orientation of the (tetragonal) crystal. In the direction of the major axis they are higher than in either of the two transverse axes: the indexes of refraction are 2.903 and 2.661 (for light of the wavelength of the D-line) and the respective values of the dielctric constant are 172 and 86 (as measured on a large crystal of the mineral rutile). In a close-sintered specimen ¹), which will contain a large number of arbitrarily oriented small crystals, an average value of approximately $(172 + 86 + 86) : 3 = 115$ may be obtained for the dielectric constant, but in actual practice it is very difficult to reach this figure. In the first place a titanium dioxide compound sintered to such an extent as to seal effectively all the pores on the surface will still contain air-occlusions at the crystal faces, and this has the effect of reducing considerably the apparent dielectric constant. Moreover, such a compound inevitably contains certain impurities, the dielectric constant of which is generally on the low side, so that in actual fact the dielectric constant ε of technical mixtures is generally lower than that of the pure titanium dioxide. If an impurity becomes dissolved in the titanium dioxide lattice, producing mixed crystals, it is not immediately clear why this should produce such a marked effect in the way of a decrease in the value of ε, but if the impurity occurs as a secondary distinct phase, having in itself a much lower ε-value, then as a rule the dielectric constant of the

---

¹) Vide R. A. IJdens, Ceramics and thier manufacture, Philips Techn. Rev. **10**, 205-213, 1948/49 (No. 7).

mixture will obviously be considerably reduced by the presence of this secondary substance.

Let us suppose, for the sake of convenience, that the secondary phase occurs in the form of layers perpendicular to the direction of the electric field, so that the lines of force traverse a dielectric whose constant is alternately high and low. The example may be further simplified by taking the case of a capacitor consisting of only two layers, i.e. a flat capacitor of which the two electrodes are a distance d apart, with a dielectric comprising a layer of titanium dioxide the ε-value of which is ε_1), and another layer, in contact with it, of a substance having a low dielectric constant (ε_2) and a thickness of xd. According to the theory of dielectrics, the field in a capacitor of this kind will conform to the requirement that the product of field strength and ε must be constant throughout. The potential difference V betweeen the two electrodes is then divided (see *fig. 1*) into two parts V_1 and V_2, so that:

$$\frac{V_1 \varepsilon_1}{(1-x)d} = \frac{V_2 \varepsilon_2}{xd} = \frac{V\varepsilon}{d}, \quad \dots\dots \quad (1)$$

where q is the apparent dielectric constant of the whole. Since $V = V_1 + V_2$, expression (1) gives us:

$$\frac{1}{\varepsilon} = \frac{1-x}{\varepsilon_1} + \frac{x}{\varepsilon_2}. \quad \dots\dots\dots \quad (2)$$

Let $\varepsilon_1 = 100$ and $\varepsilon_2 = 5$. The following values of ε will then be found in relation to x:

x	ε
0.000	110
0.005	99
0.01	91
0.05	54
0.10	36

Although this is only a very simplified example, it nevertheless demonstrates the marked reduction in the value of ε produced by the smallest admixtures in the dielectric: impurities to the extent of only about 0.5% immediately reduce the value of ε to a point below 100. Generally, such impurities are already present in the raw materials, or may be introduced in the course of the further processing. Small air-gaps between the crystals of the sintered mixture, or cavities within the mass, have an even more pronounced effect (since in that case $\varepsilon_2 = 1$). It therefore follows that the value of ε can be raised to 100 or slightly more only by taking the most stringent precautions.

It is hardly to be expected that expression (2) will provide an accurate quantitative criterion of the effect of admixtures or air-occlussions in titanium dioxide upon the value of ε, since we have based our example on an extremely simplified case which will certainly not be met with in general practice. It is possible, none the less, in the same way to construct expressions in respect of other, rather more complex examples, for instance where the one medium, in the form of ellipsoidal particles arbitrarily oriented, is enclosed within the other ²). The appropriate expression may then be readily simplified to suit spheroidal particles, more or less flat particles (in which case one dimension of the ellipsoid is small in relation to the others), or needle-like particles (with one dimension large in contrast with the others). It may be anticipated that such hypotheses would more closely approximate actual conditions.

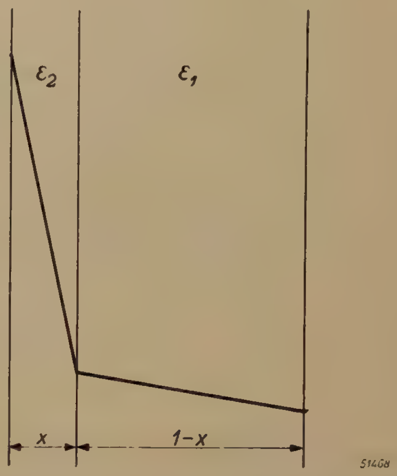

Fig. 1. Diagram showing the drop in potential in a double-layer capacitor. The thickness of the layers is indicated by xd and $(1\text{-}x)d$: the dielectric constants are respectively ε_2 and ε_1.

We are more particularly interested in the case where the secondary substance occurs in the form of flat, plate-like particles. If titanium dioxide be contaminated with a small quantity of a secondary substance it may be expected, in general, that the latter will accumulate at the crystal boundaries and thus reveal some analogy to flat particles having a low dielectric constant. When the calculation is carried out in respect of this particular case, to determine the effect of admixtures on the value of ε, it will again be found that the addition of relatively small quantities of substances having a low dielectric constant produces an exceptionally

---

²) D. Polder and J. H. van Santen, Physica, **12**, 257-271, 1946.

sharp decrease in the apparent dielectric constant of the titanium dioxide mixture.

Reasons for the high dielectric constant of TiO_2

Let us for a moment investigate the causes of the extremely high dielectric of titanium dioxide.

The dielectric constant of a substance is defined as follows: when the space between the electrodes of a capacitor is filled with an insulating substance of dielectric constant ε, the charge on the electrodes, at a given potential, is ε times as great as when that space is empty; this constant is always greater than unity. The effect of such a medium, of which $\varepsilon > 1$, upon the charge in a capacitor is an outcome of the fact that it is built up of positive and negative charge-carriers which are able to migrate among themselves but which are nevertheless limited to their positions of equilibrium.

In a substance such as TiO_2 two possibilities have to be taken into account: firstly the chemical structure is strongly polar, so that TiO_2 may be imagined, as an approximation, as being built up from Ti^{4+}-ions and O^{2-}-ions which are able to undergo a limited amount of displacement in an electric field. Each ion, moreover, consists of a positively charged nucleus within a cloud of negatively charged electrons which in turn will also move with respect to each other in an electric field.

Consequently, in a homogeneous substance every volumetric element dv will have a dipole moment $P dv$ equal to the product of the displaced charge and the distance over which the negative charge has been displaced, with respect to the positive charge. The dipole moment per cubic centimetre (the polarisation P) is nil when $\varepsilon = 1$ and is proportional to $\varepsilon-1$. Further, provided the field is not too strong, the displacement of the charge is proportional to the applied electric field E. This is expressed by:

$$P = \frac{\varepsilon-1}{4\pi} E \quad . \ . \ . \ . \ . \ . \ . \ (3)$$

The magnitude of the polarisation, and therefore also that of the dielectric constant of the material, is very closely related to the degree to which the above-mentioned charge displacement takes place in the electric field.

The atomic characteristic determining such charge displacements in the atom is what may be termed the polarisability of the atom. Let us first assume that this is the only active characteristic. In the case of a substance consisting of only one type of atom the same electric field influences each of the atoms. Suppose that the value of this field at the atom be F, then the dipole moment μ generated in the atom is proportional to F and also to the polarisability α, so that:

$$\mu = \alpha F.$$

If the number of atoms per cubic cm be N, then the polarisation is:

$$P = N\mu = N\alpha F \quad . \ . \ . \ . \ . \ (4)$$

The effective field strength in the immediate vicinity of the atom however is not identical with the external field strength as applied, since the dipoles generated in the other atoms produce an additional field. The relation between F and E within a space of cubic symmetry is rendered by:

$$F = E + \frac{4\pi}{3} \cdot P,$$

(as given by Lorentz), so that formula (3) immediately gives us:

$$F = E + \frac{\varepsilon-1}{3} \cdot E = \frac{\varepsilon+2}{3} \cdot E \quad . \ . \ . \ . \ (5)$$

Elimination of P and F from (3), (4) and (5) then finally yields:

$$\frac{\varepsilon-1}{\varepsilon+2} = \frac{4\pi}{3} N\alpha \quad . \ . \ . \ . \ . \ . \ . \ (6)$$

Expressions (3) to (6) are given in electrostatic units, but according to the rationalised Giorgi system[3]) they would take the following form:

From the formula:

$$D = \varepsilon_r \varepsilon_0 E = \varepsilon_0 E + P,$$

in which ε_0 is the (absolute) dielectric constant of a vacuum, whilst ε_r represents the (relative) dielectric constant of the material, it follows that:

$$P = (\varepsilon_r - 1) \varepsilon_0 E \quad . \ . \ . \ . \ . \ . \ . \ (3')$$

In the local field F the dipole moment is:

$$\mu = \alpha F,$$

where α is again the polarisability, but which, as will be seen presently, now has another physical dimension. If N be the number of atoms per cubic metre then:

$$P = N\mu = N\alpha F \quad . \ . \ . \ . \ . \ . \ . \ (4')$$

The relation between E, F and P is now:

$$\varepsilon_0 F = \varepsilon_0 E + \frac{1}{3} P,$$

from which, in view of (3′), it follows that:

$$F = E + \frac{\varepsilon_r - 1}{3} E = \frac{\varepsilon_r + 2}{3} E \quad . \ . \ . \ . \ . \ (5')$$

Elimination of P and F from (3′), (4′) and (5′) then gives us[4]):

---

[3]) See e.g. W. de Groot. Philips Techn. Rev. **10**, 55-60, 1948/49 (No. 2) and P. Cornelius, Philips Techn. Rev. **10**, 79-86, 1948/49 (No. 3).

[4]) See e.g. R. W. Pohl, Elektrizitätslehre, Springer, Berlin, 1943 (p. 58).

$$\frac{\varepsilon_r - 1}{\varepsilon_r + 2} = \frac{1}{3\,\varepsilon_0}\,N\alpha \; . \; . \; . \; . \; . \; . \; . \; . \; . \quad (6')$$

If we ascribe to the term α/ε_0 the form α', then (6′) can be written as:

$$\frac{\varepsilon_r - 1}{\varepsilon_r + 2} = \frac{1}{3}\,N\alpha' . \; . \; . \; . \; . \; . \; . \; . \; . \quad (6'\text{a})$$

The quantity α', as also α in (4) and (6), has the dimension of a volume; on the other hand, α in (4′) and (6′) bears the dimension

$$\text{A·sec·m : V/m} = \text{A·sec·m}^2/\text{V}$$

Indicating the term α in (4) and (6) by α_{esu}, we have:

$$\alpha' \ldots (\text{m}^3) = 4\pi \cdot 10^{-6}\,\alpha_{\text{esu}} = 1.26 \cdot 10^{-5}\,\alpha_{\text{esu}} \ldots (\text{cm}^3)$$

and

$$\alpha \ldots (\text{A·sec·m}^2/\text{V}) = \frac{10}{c^2}\,\alpha_{\text{esu}} = 1.11 \cdot 10^{-16}\,\alpha_{\text{esu}} \ldots (\text{cm}^3)$$

(c = speed of light in m/sec = $2.99776 \cdot 10^8$).

The second term of expression (6) is designated as p_e, in which the index e indicates that the electrons are displaced in the atom. From the derivative it thus follows that the dielectric constant is determined by a term p_e which is proportional to both the number of atoms N per cubic cm and their polarisability α. In a substance such as TiO_2, which is composed of two kinds of atoms, p_e is governed by the polarisability of the Ti^{4+}-ion and the O^{2-}-ion together. Thus, N is the number of TiO_2 "molecules" per cubic cm and α is the sum of the polarisability values of the individual atoms.

The dielectric constant in question, being determined exclusively by the displacement of the electrons in the atoms with respect to the nucleus, may be measured in an alternating field of so high a frequency that displacement of the ions in respect to each other does not take place: for this purpose electromagnetic waves at a frequency higher than about 10^{13}, i.e. of visible light, can be employed, so that it is permissible to use Maxwell's law:

$$\varepsilon_{\text{opt}} = n^2,$$

where n is the index of refraction of the substance having ε_{opt} as the optical dielectric constant.

Conversely, it is possible to proceed from the index of refraction to obtain some idea of the magnitude of p_e and α. For TiO_2 the average value of n is about 2.74. As far as the electronic contribution to the polarisability is concerned, TiO_2 should therefore have a value of $\varepsilon_{\text{opt}} = 7.5$. Applying formula (6) in this case [5]), p_e would then be $6.5/9.5 = 0.68$.

It is necessary, further, to take into account the polarisation arising from the displacement of the ions with respect to each other, and in this case we can similarly define a term p_i; hence:

$$\frac{\varepsilon - 1}{\varepsilon + 2} = p = p_e + p_i.$$

It will now be clear that in a substance such as TiO_2, of which the index of refraction is already relatively high, the part played by p_i in the total value of p — in comparison with p_e — need be only small in order to yield a high value of ε, since, if $p = 1$, the value of ε would already be infinitely high. From the experimental value of $\varepsilon = 110$ it follows that in the case of titanium dioxide $p = 0.97$, which is a close approximation of $p = 1$. For the contribution in respect of the ion displacement we now have $p_i = 0.29$, which, compared with the polarisability of other ion crystals, may be considered normal.

Our conclusion is that the high dielectric constant is due to the combination of a high index of refraction n and the fact that the value of p_i is not too low.

The dielectric losses of titanium dioxide and the effects of admixtures

It now having been ascertained that ε is high in the case of TiO_2 in the pure state and that admixtures result in a sharp decline in this value, the obvious aim will be to maintain the greatest possible purity in the preparation of this substance, before processing it in the form of ceramic material. This, however, is easier said than done, for the preparation and processing of TiO_2 involves a number of difficulties, added to which is the fact that a high value of ε is not the only requirement to which insulating materials have to conform. In many cases it will be found that admixtures to the TiO_2 are unavoidable.

When TiO_2 is to be used as basic material for capacitors there is no doubt that a high value of ε is very important, but it is also essential that the dielectric losses shall be low, especially in cases where the capacitor is to be employed in circuits working on high frequencies. The amount of these dielectric losses is customarily expressed as the value of $\tan\delta$, in which δ represents the angle of loss. Material which is to be employed for high-frequency capacitors usually has to conform to a value of $\tan\delta$ not exceeding 10^{-4} to 10^{-3} [6]).

---

[5]) Admittedly this is not strictly correct, since the crystal lattice of TiO_2 does not conform to the condition that the encompassment of each ion shall be cubic-symmetrical. Nevertheless, it is quite feasible to apply this formula as an approximation, especially considering that we are employing the average value of n^2 (average of the three crystal planes). The difference is not so great as to affect the final conclusion in any way.

[6]) For comparative purposes the average value of $\tan\delta$ with respect to certain non-ceramic insulating materials may be noted, viz: mica 1×10^{-4}, ebonite 81×10^{-4}, paper 140×10^{-4}, celluloid 450×10^{-4}.

Material prepared from reasonably pure titanium dioxide has a high value of ε, but its dielectric losses are intolerably high, partly owing to the high sintering temperature and its pronounced tendency at this temperature to evolve oxygen and revert to lower oxides, such as Ti_2O_3, which are semi-conductors [7]) and therefore useless for dielectric purposes. Even the smallest proportion of such oxides, too small to be determined by chemical analysis, will be sufficient to increase the loss factor $\tan\delta$ far beyond the permissible limit. This reducing effect becomes all the more marked according as the surrounding gases during the firing contain less oxygen and greater proportions of reducing agents.

It is, however, difficult to avoid these unwanted constituents. Owing to the dissociation just mentioned, it is impossible to indicate the melting point of titanium dioxide with any accuracy, but it is certainly above 1700 °C. A temperature of about 1500 °C — which is relatively close to the melting point — is therefore necessary to sinter the material closely, and such high temperatures are best obtained by gas firing, in the large kilns generally employed in the ceramic industry. It will be readily understood, then, that the exclusion of reducing gases from the firing space is an extremely difficult matter; in fact, when titanium dioxide material is fired in a gas kiln considerable reduction does actually take place.

One way of counteracting this effect it to add other substances to the TiO_2. Several substances, for instance clay, reduce the sintering temperature of the mixture, so that these lower oxides are not so easily formed. Various substances will, moreover, decrease the tendency towards the actual reduction itself, and in this way a raw material can be produced the loss factor of which is within the prescribed limit. In the meantime, however, ε will be found to have dropped as low as 60 or 80. Efforts have therefore to be made to evolve a composition, as well as a method of preparation, which will ensure satisfactory values both of ε and $\tan\delta$. It has been found possible in some cases to effect this by cooling the fired product in such a way as to introduce re-oxidation and thus nullify the reducing effect of the sintering process; this may be done by re-heating to a slightly lower temperature (about 1200 °C) in air or, even more simply, by retarding the cooling of the titanium dioxide products after the normal sintering. In this way a temperature zone is passed through in which the oxygen dissociation-pressure of the material is sufficiently low to permit of the re-formation of stoichiometrically pure titanium dioxide, the reaction rate remaining high enough to allow this re-formation to take place within the space of a few minutes. None the less, from the fact that the two measures referred to do not always yield the desired result, or at any rate not to a sufficiently high degree, it follows that the above mentioned partial reduction of the material is not the only source of a high loss factor.

There is no certainty regarding the origin of the dielectric losses occurring in the purest possible TiO_2 after full re-oxidation has been assured, but means have been found to limit these losses to a considerable extent by observing certain special precautions in the processing of the product. The first of these essential, is a rapid cooling after sintering and subsequent re-oxidation to stoichiometric TiO_2, which means that the sintered product is first cooled slowly to about 1100 °C, after which the cooling rate is accelerated.

The fact that we can obtain in this way a material with a low loss factor has led to the assumption that the previously mentioned dielectric losses (which appear to be present after complete re-oxidation) must be ascribed to the presence of impurities in the material. Closer investigation has shown, in fact, that traces of alkali metals (Na, K), and especially alkaline earth metals (Ca, Ba), have a very adverse effect on the dielectric losses.

Once this was known, a second method of reducing the loss factor to within the proper limits was made available to us. We therefore start with the purest possible titanium dioxide, in which the content of the deleterious oxides mentioned has been reduced to the technical minimum and in which the effects of any remaining unwanted oxides have been neutralised by the addition of small quantities of other oxides. It might be argued in spite of this, as mentioned above, that even one or two tenths of one per cent of impurities would be enough to reduce the dielectric constant from 110 to less than 100, but in actual practice the method in question has yielded satisfactory results. By basing the product on TiO_2 which is extremely pure by technical standards, so that any necessary additions may be limited to a minimum, it has been found possible to produce a titanium dioxide having an ε-value of 100 to 105, with $\tan\delta$ at most a few times 10^{-4} (at a frequency of 1500 kc/s).

It is a noteworthy fact, too, that the method in question enables us to obtain a ceramic material the loss factor of which is low not only at 1500 kc/s but also at 10 kc/s. If use is made of TiO_2

---

[7]) See article by E. J. W. Verwey, Electronic conductivity of non-metallic materials, Philips Techn. Rev. 9, 46-53, 1947 (No. 2).

containing a large percentage of clay the most favourable case will yield dielectric losses which are low at 1500 kc/s but high at 10 kc/s, as demonstrated in *fig. 2,* in which tanδ is shown plotted as a function of the frequency, with the two different mixtures as parameters.

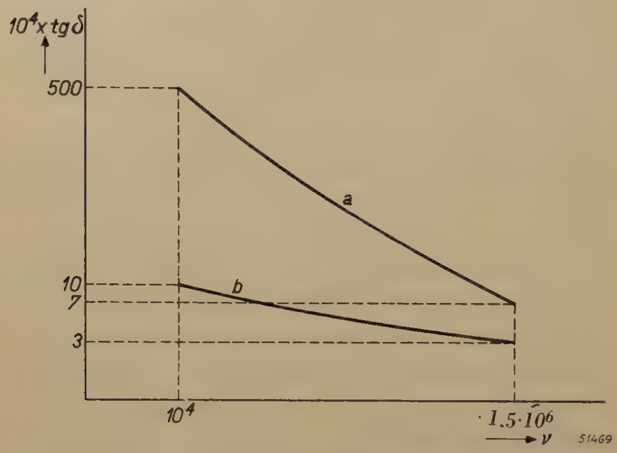

Fig. 2. The value of tanδ as a function of the frequency of the alternating current applied. The frequency ν of the current in c/s and the value of tanδ are shown plotted on logarithmic co-ordinates. Curve *a* refers to titanium dioxide to which a high percentage of clay has been added, and curve *b* to technically pure TiO_2 in which the inevitable impurities, of oxides of alkaline-earth metals, have been neutralised by small quantities of other oxides.

Temperature coefficient of the dielectric constant

Once it has been assured, by a careful choice of the composition and the method of preparation of the ceramic material, that the final product will have a high value of ε and a low tanδ, attention must be paid to a final factor, the temperature coefficient of the dielectric constant, for, in the case of titanium dioxide, the value of ε is very highly dependent on the temperature. Curiously enough, this temperature coefficient, in contrast with that of nearly every other material, is negative, i.e. $1/\varepsilon \cdot \mathrm{d}\varepsilon/\mathrm{d}T = -8.10^{-4}$. This means that an increase of, say, 12.5 °C in the temperature of a capacitor having TiO_2 as dielectric causes the capacitance to decrease by 1%.

In certain applications such a high coefficient is a decided disadvantage. Take as an example the case of a capacitor in the tuning circuit of a radio receiver tuned at room temperature to a given station: as soon as the capacitance changes, which it will do after a little while owing to the increase in the working temperature of the set, the tuning will be upset. On the other hand there are cases where the high negative temperature coefficient may prove an advantage in compensating the coefficient in other components in the circuit, which is usually of the opposite sign.

It may well be asked what the relation is between the temperature coefficient of the dielectric constant and the other characteristics of titanium dioxide. According to expression (6), the temperature coefficient of ε is determined by that of $N\alpha$. Clearly, as a result of the thermal expansion the number of atoms per cubic cm decreases as the temperature is raised; in other words, the dielectric constant decreases with rising temperature. This effect may be counteracted by the variation in α with T, but in the case of a substance such as TiO_2 it appears that the value of α as calculated from the rather approximate formula (6) depends very little upon the temperature, so that the temperature coefficient of ε is determined almost wholly by the thermal expansion. At high values of ε, small variations in N result in relatively marked changes in ε, as will be seen from the relationship between these quantities in accordance with expression (6). The high temperature coefficient of TiO_2 is thus directly related to the high value of ε.

In the case where $\mathrm{d}\varepsilon/\mathrm{d}T \approx 0$, as roughly approximated in TiO_2, the following may be derived from formula (6):

$$\frac{1}{\varepsilon} \cdot \frac{\mathrm{d}\varepsilon}{\mathrm{d}T} = \frac{(\varepsilon-1)(\varepsilon+2)}{3\varepsilon} \cdot \frac{1}{N} \cdot \frac{\mathrm{d}N}{\mathrm{d}T} \quad . \ . \ . \ . \ . \ (7)$$

If we introduce an average linear coefficient of expansion:

$$\beta = -\frac{1}{3N} \cdot \frac{\mathrm{d}N}{\mathrm{d}T}$$

expression (7) may be written in the form:

$$\frac{1}{\varepsilon} \cdot \frac{\mathrm{d}\varepsilon}{\mathrm{d}T} = -\frac{(\varepsilon-1)(\varepsilon+2)}{\varepsilon} \beta \, , \quad . \ . \ . \ . \ . \ (8)$$

which, at high values of ε, becomes:

$$\frac{1}{\varepsilon} \cdot \frac{\mathrm{d}\varepsilon}{\mathrm{d}T} = -\beta\varepsilon \quad . \ . \ . \ . \ . \ . \ . \ . \ (9)$$

The temperature coefficient is thus negative in such substances and is also proportional to the average linear coefficient of expansion.

It is necessary here to stress the fact that there are also many substances, especially those whose dielectric constant is low, in regard to which variations of α with the temperature also play a part.

It has already been mentioned that the high negative temperature coefficient is a disadvantage in many applications of the material in question. By adding other substances having a positive temperature coefficient it is possible to produce a mixture the temperature coefficient of which is very low, or even zero, but this can be done only at the cost of a high value of ε, as may be expected in the light of the remarks made in the opening paragraphs of this article. Let us now look at one or two examples of ceramic mixtures of this kind.

For many years MgO has been known as a suitable constituent; the sintered product in this case yields a material consisting in part of magnesium titanate, and provided the proportions are suitably chosen $1/\varepsilon \cdot \mathrm{d}\varepsilon/\mathrm{d}T$ is for all practical purposes zero. The dielectric losses of this material are very low ($\tan\delta = 1 \times 10^{-4}$ at 1000 kc/s) but the dielectric constant is not much more than 12 to 18.

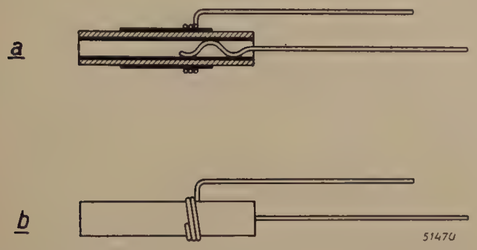

Fig. 3. Type "A" ceramic capacitor: *a* cross section, *b* side view. The length varies between 15 and 40 mm, whereas the capacitance may be from 33 to 1200 pF. The electrodes comprise two silver layers, the inner connecting lead being mounted by pressing the spiralized extremity into the ceramic tube.

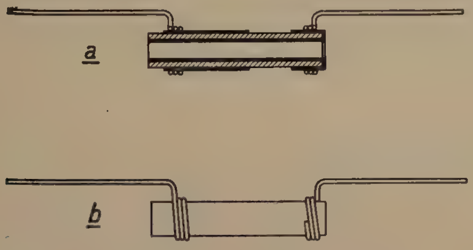

Fig. 4. Type "B" ceramic capacitor. *a* section, *b* side view. Dimensions are the same as for type A. In this case the lead connected to the inner electrode is mounted on the outside.

Another method consists in the addition of steatite, which will also give an ultimate temperature coefficient of 0, with very low losses, but ε is then only about 10.

Philips have developed a special mixture, using CeO_2 as a constituent. It was found that the dielectric constant of this substance is still fairly high, viz. about 35, whilst the temperature coefficient, dependent to some extent on the purity of the oxide, is generally weakly positive [8]). Therefore, mixtures prepared from CeO_2 and TiO_2, the temperature coefficient of which is to be roughly zero, must contain a very large proportion of CeO_2, a typical example being 85 mol% CeO_2 and 15 mol% TiO_2. This mixture is thouroughly sintered at 1220 °C, a temperature very much lower than that required for pure TiO_2. The dielectric constant is approximately 40, with $\tan\delta$ approx. 8×10^{-4} at 1000 kc/s.

Another possibility which we have investigated concerns admixtures of SnO_2. 50 mol% SnO_2 and 50 mol% TiO_2 yields a temperature coefficient of roughly zero. The firing temperature is certainly very high, being 1550 °C, but the losses are extremely low ($\tan\delta \approx 1 \times 10^{-4}$ at 1000 kc/s), whilst for the mixing ratio in question ε is 25.

Finally, mention should be made of ZrO_2 as a possible constituent: this may be introduced in a number of ways. In the first place, if not more than 1 or 2 % zirconium oxide is added, $\varepsilon \approx 60$ and $\tan\delta \approx 5 \times 10^{-4}$ at 1000 kc/s, but $1/\varepsilon \cdot \mathrm{d}\varepsilon/\mathrm{d}T$ is then still markedly negative (-6×10^{-4}). Alternatively, the admixture of ZrO_2 can be increased until $1/\varepsilon \cdot \mathrm{d}\varepsilon/\mathrm{d}T$

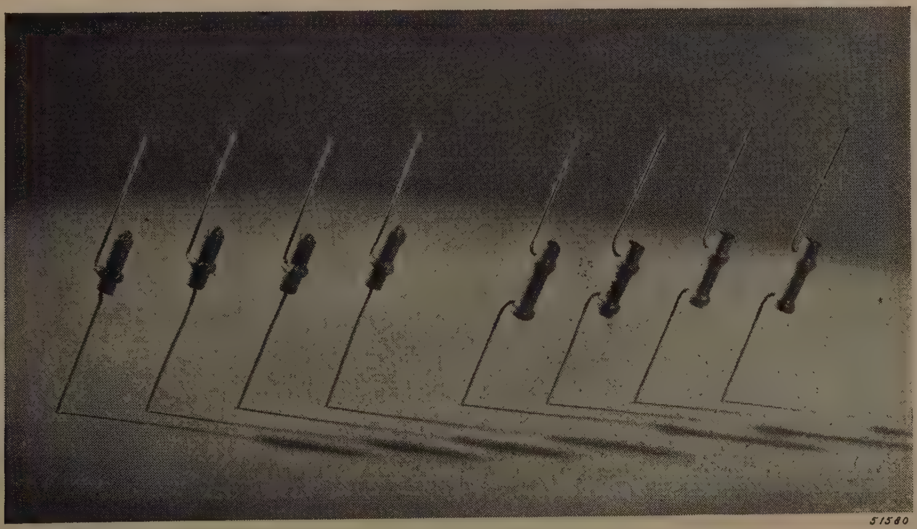

Fig. 5. Two groups of ceramic capacitors as supplied ready for use. On the *left* 4 capacitors of the "A" type; on the *right* the "B" type.

---

[8]) The spreading of the values is related partly to the losses. According to the rule of Gevers and du Pré (Philips Techn. Rev. 9, 91-96, 1947, (No. 3), for this material that contribution towards the temperature coefficient which is related to the dielectric losses is roughly equal to $0.06 \tan\delta$: at $\tan\delta = 10^{-3}$ this is therefore $+ 0.6 \times 10^{-4}$.

≈ 0, but, although this shows the same dielectric losses, ε will be found to have dropped to the order of 30. In this case, moreover, a high sintering temperature is needed.

From these examples it will be seen that variations in the ceramic mixtures will produce widely divergent dielectric properties, and it is on the basis of these experimental results that the composition of ceramic materials is determined, to meet the particular requirements to which any given product may have to conform.

Capacitors made of ceramic material

We close the present article with a brief reference to one particular application of ceramic materials for capacitors: these comprise a range of miniature capacitors for which a high dielectric constant is required to suit the capacitance values concerned. *Figs 3* and *4* show the method of construction.

These components, the length of which varies from 15 to 40 mm [9]), are manufactured in capacitances varying from 33 to 1200 pF. The tolerance ranges are 20, 10, 5 and 1%, although the maximum guaranteed accuracy is ± 1 pF. The maximum working voltage is 600 V, but each capacitor is factory-tested on 1500 V, A.C. 50 c/s, for 1 hour. As far as the dielectric losses are concerned, $\tan\delta$ is less than 20×10^{-4} in the "A" type (at 1500 kc/s) and less than 10×10^{-4} in the "B" type. The insulation resistance is higher than 5000 megohms. On the score of mechanical strength it may be said that the ends of these small capacitors can be loaded to the extent of 2 kg without rupture.

Fig. 5 illustrates a group of these components. These may be employed in radio receivers and other high-frequency circuits.

---

[9]) In the very low capacitance values (3.3 to 27 pF, similar capacitors are made with glass as dielectric. The dimensions then lie between 15 and 30 mm.

A TRANSMITTING VALVE COOLER WITH INCREASED TURBULENCE OF THE COOLING WATER

by M. J. SNIJDERS.

621.396.694.032.42

Although air-cooling has certain advantages for transmitting valves, water-cooling has the preference where the most intensive cooling effect is required, for example in transmitters working on very short waves. It appears that considerable improvement on the usual methods of cooling can be obtained by increasing the turbulence of the water in the cooler. One very effective method of achieving this is to inject the water into the cooler by means of concentric rings with jets arranged round the anode; the jets of water set up considerable turbulence in the water within the cooler. This method has been adopted for valve types PAW 12/15 and TAW 12/35, as it has been found in practice that, above a certain anode temperature (about 90 °C), a layer of copper oxide forms on the surface of the anode, which is such a poor thermal conductor that the latter tends to become overheated. In comparison with the old type of cooler, for the same flow of water per minute and the same dissipation, the spray method results in the peak anode temperature remaining about 40 °C lower and therefore well below the critical value of 90 °C. The dimensions of both types of cooler are the same and the new system can therefore be easily incorporated in existing equipment. The increased cooling effect provided by the system under review offers the possibility of obtaining a given transmission power from smaller valves than heretofore and/or at lower wavelengths.

Transmitting valves whose dissipation lies above a certain value are usually artificially cooled, this having the effect of considerably reducing the minimum practical dimensions of a given valve; this dissipation value lies at about 3 kW.

In most cases this cooling is effected by arranging for a flow of water along the anode, which constitutes part of the wall of the valve itself (*fig. 1*). According to another method, which is being applied more and more of late, air is blown along the anode, in this case provided with suitable cooling fins. In an earlier issue of this journal ¹) a description was given of a new form of cooling fins and a special method of air distribution which will permit of air-cooling even with the largest transmitting valves. As pointed out in that article, air-cooling has certain distinct advantages over water-cooling and there can be no doubt that it will supersede the latter in many instances. Nevertheless, water-cooling will often be given preference, especially when the valve is to operate on the higher frequencies, in which case the ratio of output power to dissipated power is much less favourable than on the lower frequencies. Furthermore, at very high frequencies, capacitances have to be kept as low as possible, not only between the electrodes in any one valve, but also between the anodes of two valves in a push-pull circuit, mounted close together for compactness. All this means that every effort is made to keep the dimensions of both valve and cooler as small as possible; as far as the valve itself is concerned, this in turn leads to high specific loads (i.e. dissipation per sq. cm anode area) and therefore also highly efficient cooling. As regards the latter, the water-cooler has the advantage of its smaller dimensions in comparison with the air-cooler, so that, if the maximum dissipation of the anode is demanded, water-cooling will be preferred. In the following we propose to discuss the new method of cooling more fully.

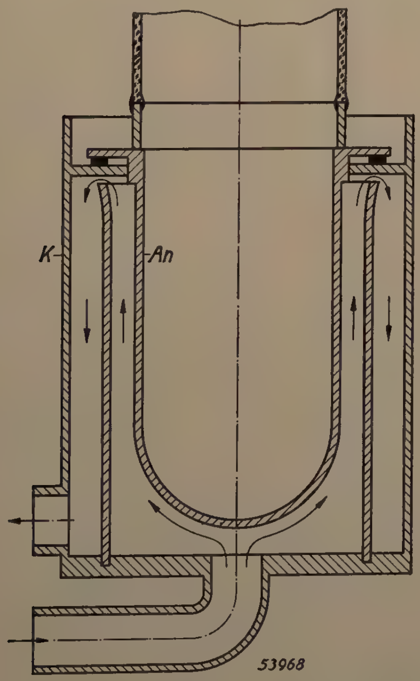

Fig. 1. *An* = anode of transmitting valve mounted in cooler *K* through which water flows.

---

¹) H. de Brey and H. Rinia, An improved method for the air-cooling of transmitting valves, Philips Techn. Rev. 9, 171-178, 1947 (No. 6).

Open and closed cooling systems

In an "open" system the used cooling water is allowed to run to waste.

In the closed system the used water, the temperature of which has been raised, is cooled down in a special cooling device and used again; in other words a fixed quantity of water is kept in circulation.

For medium-sized transmitters, in which the water consumption is not very high, the simplest form of cooling system, i.e. the open type, is usually adopted, provided the quality of the available water supply is good enough, that is to say sufficiently free from elements that tend to fur the anodes, (this point will be referred to in detail later). Boiler scale is a very bad conductor of heat and therefore reduces the cooling effect, with the result that the valve ultimately runs the risk of being overheated. If only "hard" water is available then the closed system, where all the injurious constituents forming the scale speedily disappear, will have to be used. Moreover, even the initial deposit can be avoided by filling the cooling system with distilled water; it is only necessary to top up the water occasionally, to make good the small losses due to evaporation and leakage.

In large transmitters, requiring for instance a flow of water of about 500 litres (100 gallons) per minute, the closed system will always be preferable in view of the saving to be made on the cost of the pure water required for the open system.

Various methods are available for use in connection with the "return cooling" of the used water: small installations mostly employ an equipment very similar to the cooling system of a motor-car; in the larger transmitting stations use may be made of cooling towers, reservoirs or surface coolers in which the circulating (primary) water imparts its heat to running (secondary) water. The latter solution is shown in *fig. 2* (the closed type of system employed in the main Netherlands broadcasting stations).

The purity of the secondary cooling water need not be particularly high, as experience has shown that deleterious substances are not deposited in the return cooler, this being due to the fact that the temperature of the primary water is fairly low (at most 30 °C). The secondary supply may therefore consist of unpurified well-water, which is comparatively cheap.

Another advantage of the closed system, provided distilled water is used, is evident from what follows. The anode of the transmitting valve to be cooled carries a very high D.C. potential with respect to earth (possibly 20 kV) and also a high superimposed h.f. alternating voltage. Now, for the purposes of electrical insulation, the cooling water for the anode is fed and carried away through long insulating tubes. In order to save space these tubes (preferably made of ceramic material) are usually arranged in the form of a coil (*S* fig. 2). Although the tubes themselves are non-conductive, there is nevertheless a certain leakage of current through the stream of water. This loss can be limited to a minimum by filling the closed system with distilled water, which has a low conductivity. The efficiency of the transmitter is thus considerably improved.

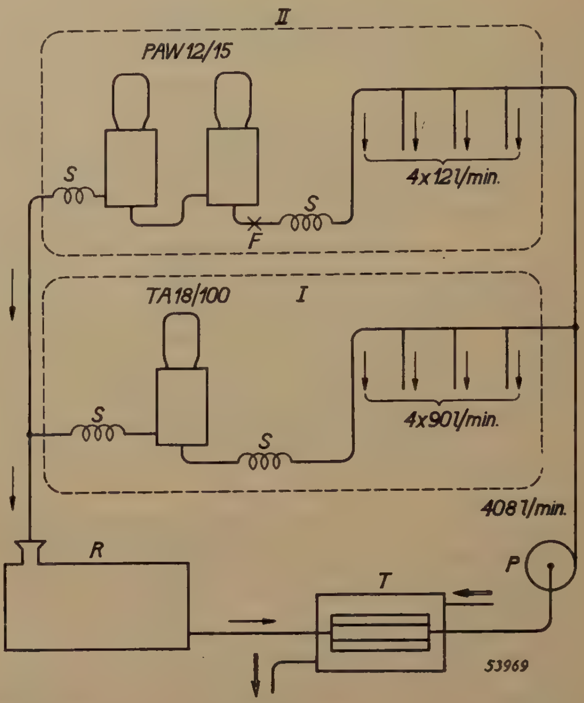

Fig. 2. Diagram of the closed cooling system as employed in the Netherlands broadcasting stations. The flow of the primary water is indicated by single arrows; that of the secondary water by double ones. *P* = pump, *I* = output stage, *II* = driver stage, *S* = coiled ceramic tube (for electrical insulation), *R* = reservoir, *T* = return cooler.

The output stage (*I*) comprises four valves type TA 18/100, plus two reserve valves not shown in the diagram. When the latter are put into service the cooling water is switched over simultaneously with the electrical connections. The driver stage (*II*), incorporating four PAW 12/15 valves, is arranged differently: in this case the cooler of each of the functional valves is connected in series with that of the associated reserve valve. In the figure only one of the four pairs is shown. At the point *F* a filter may be fitted (to be discussed later).

Possible causes of deposit on the anode

We have already mentioned the possibility of furring in the case of the open cooling system. It might be inferred, in view of the foregoing, that there would be no questoin of any kind of deposit in a closed cooling system containing distilled water, but in practice furring does actually take place, owing to the circulating water picking up substances from the walls of the system, thus forming compounds which are deposited on the anode. For example, if the water is in direct contact with concrete, as may be the case if a reservoir as represented in fig. 2 is used, boiler scale will form on the anode; such reservoirs should therefore always be lined with chlorinated rubber paint to prevent the water from coming into direct contact with the concrete.

It has been found at a number of transmitting stations that, even though such precautions are taken and distilled water is used, a heat-insulating deposit — albeit not boiler scale — tends to form on the anode. In fact a hard, black deposit has been found on the anodes of the PAW 12/15 and TAW 12/35 (*fig. 3*) as employed in different broadcasting stations where closed cooling systems were in use; this layer proved to be copper-oxide (CuO), which, although not such a poor conductor of heat as scale, may nevertheless lead to overheating of the valve.

Measures to prevent the deposit of copper-oxide

These copper-oxide deposits can of course be removed from time to time by sanding or pickling, but such operations, involving as they do the dismantling of the valve and subsequent re-inserting in the cooler, incur considerable risk of breakage (not only of the glass, but also of the tungsten filament, which in time becomes brittle).

One way of preventing the occurrence of copper-oxide would be to arrange matters so that at least one of the elements of which it consists cannot appear at the anode. Since the water is exposed to the air at a number of points (as in the reservoir, see fig. 2), the solution of oxygen can hardly be prevented. The presence of copper itself is even more difficult to avoid, as in the first place the anode is made of this material and, moreover, the whole cooling circuit, pumps, cocks and other equipment must necessarily consist of non-corroding material. Tinning of such components, as well as of the anode itself, would effectively prevent all direct contact between copper and water, but we found a much simpler method of preventing the formation of copper-oxide, consisting in a reduction in the temperature of the anode by intensifying the cooling. An improved type of cooler, which forms the subject of the present article, has been specially developed for this purpose.

In fact there are a number of indications that a reduction in the anode temperature reduces the formation of copper-oxide and that below a certain temperature limit it is almost entirely absent. The indications in question, as observed in a number of broadcasting stations, are the following:

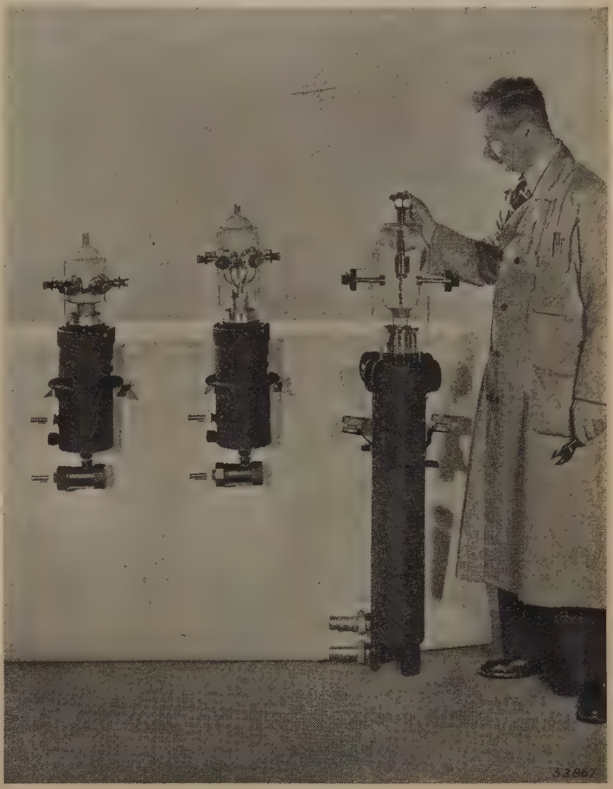

Fig. 3. The three transmitting valves mentioned in this article. From left to right: the pentode PAW 12/15, the triode TAW 12/35 and the triode TA 18/100.

1. Copper-oxide appeared more abundantly at the hottest parts of the anode.
2. More copper-oxide per unit of time was produced in heavily loaded valves of the type PAW 12/15 than in the more lightly loaded valves.
3. Type TA 18/100 valves (fig. 3) as used in the same transmitter and employing the same cooling water as the two previously mentioned PAW 12/15 valves (see fig. 2) showed no copper-oxide deposit, even under the heaviest loads. In fact, the anode temperature of the valves TA 18/100 appeared to be lower in this case than that of the valves PAW 12/15, as was proved by provisional measurements by means of thermo-couples soldered to the anodes. For the results of the measurements see *table I*. (For practical reasons these measurements were carried out under static load [2]), calcu-

---

[2] The temperature under static load is less uniformly distributed over the anode than in the case of dynamic loading. This point is dealt with more fully in connection with the more accurate measurements described in the following paragraphs; the values given in table I are the outcome of less provisional, precise measurement.

lated to give the same dissipation as in the most heavily loaded valves in the transmitter.

The formation of copper-oxide appeared to cease at temperatures between 55 and 94 °C; according to later measurements the actual limit is in fact about 90 °C.

Table I. Measured temperatures of transmitting valves. t', t'' = temperature of cooling water at inlet and outlet of the cooler respectively, A = flow of water, P_{tot} = total dissipation calculated from $t''-t'$ and A, t_a = anode temperature measured with thermo-couple (roughly at the hottest place).

Type	PAW 12/15	TA 18/100
t' (°C)	20	20
t'' (°C)	30	26
A (l/min)	12	90
P_{tot} (kW)	8.4	37.7
t_a (°C)	94	55

The cooling of the valve PAW 12/15 in comparison with that of the valve TA 18/100

The problem, therefore, was how to keep the anode of the PAW 12/15 at a sufficiently low temperature.

The differences in the anode temperature as shown in the above table are not to be accounted for by the specific anode load of the PAW 12/15 in that particular transmitter being higher than that of the TA 18/100, for as a matter of fact the specific load on the PAW 12/15 was 23 W/cm² and that on the TA 18/100 26 W/cm².

The reason for the difference in temperature is apparent, however, when the speeds of flow of the water are compared: this speed, v, is obtained from the quotient of the flow A and the cross-sectional area O of the annular water-jacket surrounding the anode. In both cases O was 10.6 cm²,and the values of A, as shown in the table, were 12 and 90 l/min, or 0.2×10^{-3} and 1.5×10^{-3} m³/sec respectively, so that, for the PAW 12/15:

$v = 0.2 \times 10^{-3}/10.6 \times 10^{-4} = 0.19$ m/sec.

and for the TA 18/100:

$v = 1.5 \times 10^{-3}/10.6 \times 10^{-4} = 1.4$ m/sec.

In the case of a laminary flow of cooling liquid over a heated surface the transfer of heat from the latter to the liquid takes place exclusively by conduction (radiation may be ignored here); now, the coefficient of thermal conductivity — i.e. the amount of heat transferred to the cooling agent per unit of the surface area, per unit of time and per degree difference in temperature — is independent of the rate of flow of the medium.

However, even at the lower of the two above-mentioned speeds the flow of water is turbulent and the volume elements of the water therefore acquire a component of speed in a radial direction as well as axial speed v as calculated above; the hotter volume-elements are thus transported to the colder places and vice versa. Due to this radial component convection occurs, as a result of which the coefficient of thermal conductivity is much greater than when attributed to conduction only. Furthermore, turbulence in the water involves another factor, in that, owing to the eddies, each aqueous element may come into repeated contact with the surface to be cooled, taking up an amount of heat each time. Thus the stronger the turbulence, the smaller the differences in temperature occurring in a radial direction within the water-jacket.

The radial component of the speed of flow required for an efficient transfer of heat increases with the axial speed v of the water [3]). It might be possible to increase the speed in the case of the PAW 12/15, for instance by increasing the flow of water A per minute, but such a solution would be uneconomical in many respects. Another way out would be to reduce the cross-section O, but in practice there are limits in this direction considering that the anode and water-jacket are only 3 mm ($^1/_8$") apart, whilst allowance must also be made for the fact that the anode is not always perfectly cylindrical.

Other means have therefore to be sought to increase the turbulence of the water in the cooler.

The spray cooler

A very high degree of turbulence can be obtained by injecting the water into the cooler in a suitable manner, and *fig. 4* gives details of a very practical method. The water is sprayed from a number of jets placed in a ring round the anode and sets up inside the filled cooler a violent circulation the main direction of which — accompanied by subsidiary eddies in other directions — is indicated by the dotted lines in the diagram.

Fig. 5 shows the ultimate arrangement as applied to the valve PAW 12/15; a similar form of cooler has also been developed for the valve TAW 12/35. The water enters a channel at *1* which is drilled in the bronze bottom of the cooler and subsequently branches into four ducts, each of which leads to a vertical tube through which the water reaches three jet-rings. Finally, the water leaves the cooler at *5*.

---

[3]) It is actually less than proportional, e.g. in some cases proportional to $v^{3/4}$; see A. Schack, Der industrielle Wärmeübergang, Düsseldorf 1940, 2nd edition, p. 60.

The external dimensions of the cooler are exactly the same as those of the old type.

Calculations

The design of the new cooler is based on the same flow of water as the old type (12 l/min = 2.64 gallons/min = 200 cm³/sec for the valve PAW 12/15), so that it may be substituted for existing equipment without necessitating the installation of pumps for larger quantities/minute or higher pressures.

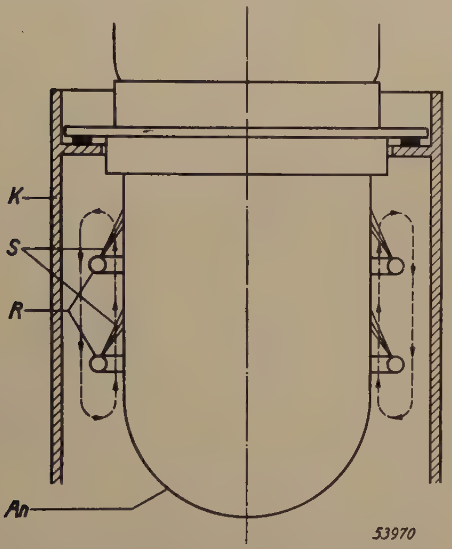

Fig. 4. Principle of the spray cooler. *R* = injector rings producing jets of water *S*, which keep the cooling water in violent motion. *An* = anode, *K* = cooling jacket.

The speed of flow of the water, v_0 (in m/sec), passing from the jets is rendered by the expression

$$v_0 = \sqrt{2gh},$$

where g is the gravitational acceleration (in m/sec²) and h the difference between the pressures (in m water column) in front of and behind the jets. If h be the total drop in pressure in the cooler — for which we maintain of the old cooling device (h = 1 m in the case of the value PAW 12/15) — the exit speed will be

$$v_0 = \sqrt{2 \times 9.81 \times 1} = 4.4 \text{ m/sec.}$$

Since there is also a certain drop in pressure in the other parts of the cooler and h is thus slightly less than 1 m, we shall assume that $v_0 \approx 4$ m/sec.

From this assumed flow of water it follows that the jets must have a total orifice area of 200/400 = 0.5 cm². The question as to the most suitable number of holes into which this area can be divided is governed by the fact that, on the one hand, a large number of holes promotes more uniform cooling, whereas on the other hand — and this is a more practical consideration — small holes are more liable to become clogged.

In view of this latter factor, a diameter of 1 mm has been taken for the jets, necessitating 60 holes to give a total area of 0.5 cm².

To eliminate any possible risk of stoppages the simple filter shown in *fig. 6* has been designed. This is fitted at the inlet of the cooler (at *F* in fig. 2).

Other points to be taken into consideration were the most suitable number of rings among which to divide the 60 jets, the most satisfactory height in respect of the anode at which to place them, the most effective angle for the jets of water, etc. These problems were solved experimentally, mainly with the aid of temperature measurements (discussed in

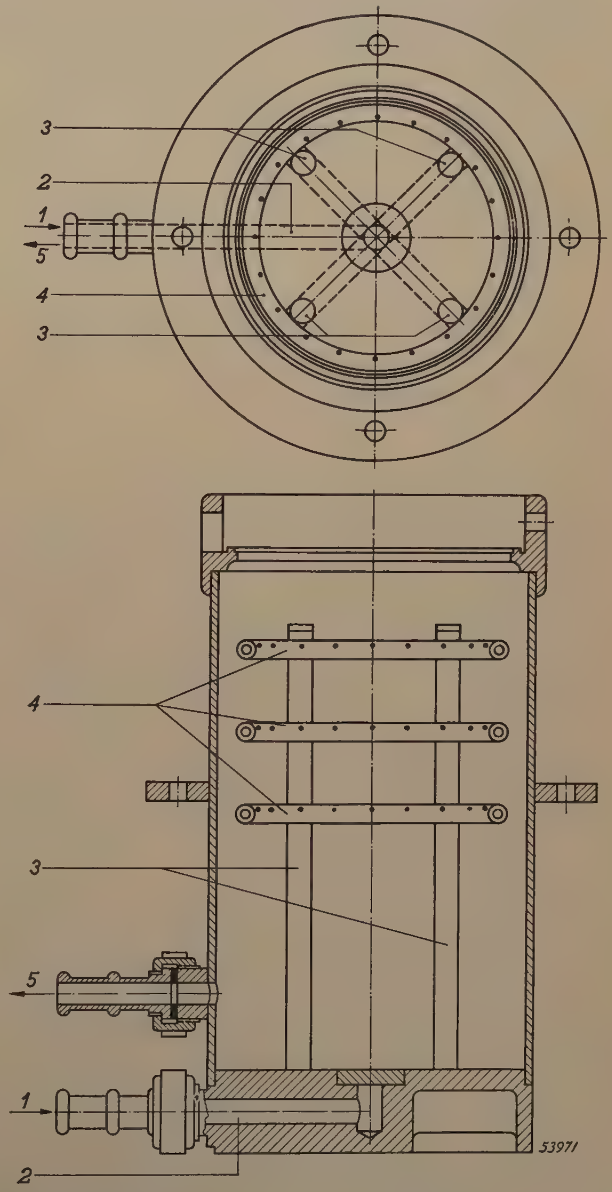

Fig. 5. Top view and vertical cross-section of the spray cooler. The cooling water enters at *1*, flows through duct *2* and branches into four tubes *3*, thus reaching the three jet-rings *4* and ultimately leaving the cooler at *5*.

the next paragraph) taken[3] with a cooler so constructed that the factors in question were variable. As will be seen from fig. 5, the number of rings has been fixed at three. The most satisfactory angle for the jets of water was found to be obliquely upwards towards the anode, at an angle of 30° from the vertical.

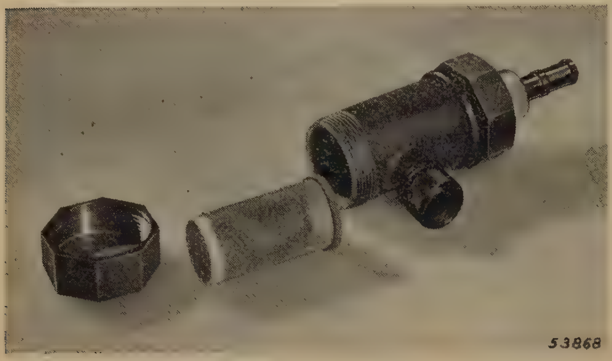

Fig. 6. Simple filter made of metal gauze. It is included in the water system at the inlet of the spray cooler (at F in fig. 2) and can be easily mounted on the latter (see left-hand and centre valves in fig. 3).

Measurements

To ensure accuracy of measurement of the anode temperature, five thermo-couples were provided along each of four longitudinal lines on the anode (*fig. 7a* and *b)*.

A few remarks may be added in regard to the place and the construction of these thermo-couples.

1) The lines on which the latter were placed were chosen exactly in the centre of the open spaces between the grid supports, for the following reason. It is very difficult to carry out temperature measurements on an oscillating valve, so that for practical reasons a static load had to be applied. The control grid is then at a steady negative potential which produces a marked shadowing or screening of the grid supports; the current density at those parts of the anode immediately behind these supports is therefore much lower than in the intervening spaces and those sections of the anode will therefore become less hot. Points of measurement were therefore decided upon lying in the centre of the open space between the supports in order to avoid taking the measurements under too favourable conditions (fig. 7*a*).

It is not sufficient to limit the measurements to only one such row of points, in view of small but inevitable asymmetries in the locations of the electrodes with respect to the anode. When the valve oscillates — under normal working conditions — the grid potential periodically assumes values in the region of zero, so that over an average period of time the effects of both the asymmetry and the screening of the grid by the supports are much less pronounced than under static load. For this reason the values indicated in the following figures are averages of the four measurements. These averages will show a fairly close agreement with the temperatures of the anode under dynamic load.

2) The thermo-couples were actually arranged in the following way in order that they might interfere as little as possible with the flow of water. At each of the points *0-5* on the longitudinal line (fig. 7*b*) a dimple was drilled in the copper anode. In each of the dimples *1-5* a thin constantan wire was soldered and at *0* a thin copper wire, the solder just filling the dimple. The six wires were insulated and carried outside through a water-tight seal in the cooler, the five constantan wires in conjunction with the copper acting as thermo-couples.

Fig. 8 shows the anode temperature of the valve PAW 12/15 plotted against the vertical distance y from the rim of the anode. The valve in question was operating at the maximum total rated dissipation of 14.25 kW [4]), with a cooler feed of 12 litres (2.6 gallons) of water per minute at 9 °C. As will be seen, the old cooler gives local temperatures in excess of 100 °C (curve *I*), whereas in the case of the new cooler (curve *II*) the highest temperature reached is barely above 60 °C.

The variation in the average temperature at the hottest part of the anode with the total dissipation is demonstrated in *fig. 9* (curve *I* for the old cooler

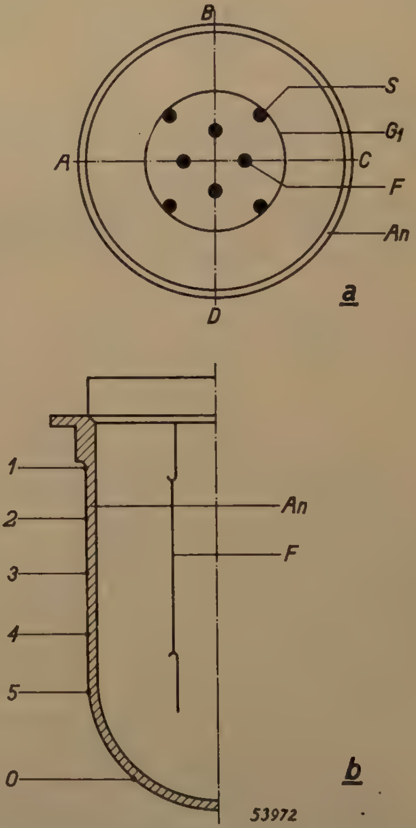

Fig. 7. (*a*) Horizontal and (*b*) vertical cross-section of the transmitting valve PAW 12/15 fitted with thermo-couples. F = filament, G_1 = control grid (not shown in *b*), S = grid supports, An = anode. Five constantan wires (*1-5*) are soldered at points along each of four longitudinal lines A, B, C and D and these, together with the copper wire *O*, form the poles of five thermo-couples.

Screen- and suppressor-grids are not shown.

---

[4]) Of which 1.83 kW is filament power, and 0.42 kW screen grid dissipation.

and curve *II* for the new type); curve *II* lies on a level which is some 40 °C lower than curve *I* and is at every point well below the critical value (90 °C) at which copper-oxide commences to form.

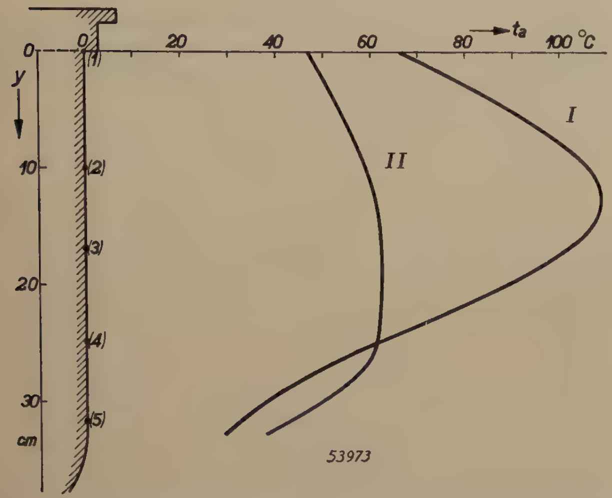

Fig. 8. Anode temperature t_a as a function of the distance y from the upper rim of the anode of a valve PAW 12/15. Curve *I* refers to the old cooler (fig. 1) and curve *II* to the spray type of cooler (fig. 5), 12 litres (2.6 gallons) of water per minute being used in each case. Total dissipation 14.25 kW. Temperature of cooling water at inlet of the cooler 9 °C, at the outlet 26 °C. The numbers (*1*)-(*5*) on the left indicate the positions of the thermo-couples.

Lines t' and t'' in fig. 9 indicate respectively the temperature of the cooling water at the inlet and outlet of the cooler.

For comparative purposes the quantity of water per minute required by the old cooler to maintain the anode at the temperature ensured by the new cooler was also measured with respect to a given dissipation: this was found to be 85 litres/min as compared with 12 litres/min in the new type of cooler.

Practical results

Comparative tests have been carried out in one of the Netherlands broadcasting stations with the PAW 12/15 valves mounted in the old and in the new type of cooler, under identical conditions of load and cooling water supply. After 170 hours operation the anode in the old type of cooler showed considerable deposits of copper-oxide, whereas the valves in the new cooler were entirely free from deposit after 4000 working hours, thus avoiding the necessity of periodical dismantling and reassembly, which is the most frequent cause of early failure of the valves.

Equally satisfactory results have been reported from another transmitting station employing TAW 12/35 valves, where heavy deposits of copper-oxide used to occur in the old type of cooler. During transmissions valves in the old type of cooler tended to "sing" loudly, indicating that the anode temperature was locally in excess of 100 °C; the normal amount of water used was 20 litres (4.4 gallons) per minute. With the new coolers the equipment was entirely free from mechanical noises and there was an entire absence of copper-oxide, although the flow of water was reduced to 16 litres (3.5 gallons) per minute, the pressure drop in the new cooler being somewhat higher than that in the old one.

After the filter shown in fig. 6 had been mounted no trouble was experienced from clogging of the jets.

Further possibilities

The introduction of the new cooler is important not only from the point of view of the increased life of the valves to which it has been adapted, but especially because this method of cooling paves the way to the design of smaller valves for a given power rating, seeing that the increased cooling effect permits of higher specific loads. This will be of advantage more especially in the case of valves working on very high frequencies, since the inter-electrode capacitances of these valves must be kept low and anode diameters small with a view to keeping the electron transit times between cathode and anode short (the transit time is one of the

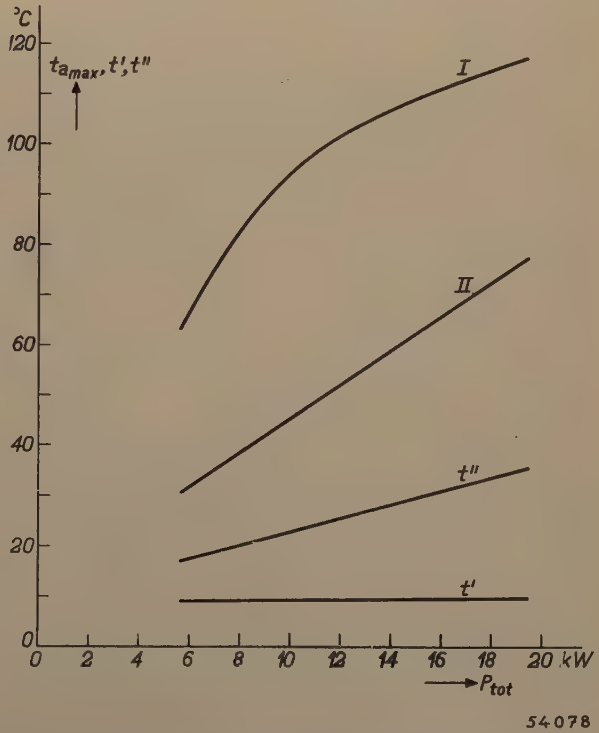

Fig. 9. Anode temperature $t_{a\,max}$ at the hottest points of measurement (*I* for the old cooler, *II* for the new one) as a function of the total dissipation P_{tot}, also temperatures t' and t'' of the water respectively at the inlet and outlet of the cooler. Flow of water 12 l/min.

factors limiting the frequencies which the valve can handle). In these cases, as far as the cooling is concerned, even better results can be anticipated than those obtained from valves PAW 12/15 and TAW 12/35 as described above, for in later types there will be more freedom in choosing the pressure drop permissible in the cooler; when a greater pressure drop is allowed than that assumed in the foregoing, more intensive turbulence and still greater cooling effects are obtainable. Since the pressure drop in the cooler always represents but a small fraction of the pressure difference required to force the water through the insulating coils, increases in this pressure drop are of little significance in comparison with the total pressure to be supplied by the pumps.

SOFT IRON FOR THE ELECTROMAGNET OF A CYCLOTRON

by J. J. WENT. 669.127.5:621.318.322

Investigation is made into the properties to be ascribed to a soft iron suitable for the construction of electromagnets as used in cyclotrons. The more important characteristics of ferromagnetic materials are first discussed, such materials being classified in four groups. A number of possible applications are then indicated for each group, after which it is shown that the iron from which electromagnets are made must possess high saturation values and relatively high remanence. Taking into consideration the general picture which ferromagnetic materials should present, it is then seen that the last-mentioned requirement can be met only when care is taken to minimise internal strains and any non-magnetic constituents that may be present. Since these desiderata are also conducive of a low coercive force, the same grades of iron can also be employed for the iron cores of relays. Finally, details are given of the conclusions drawn from this review as applied to a practical test in the manufacture of the iron used for a cyclotron built by Philips for the Institute for Nuclear-Physical Research at Amsterdam.

Introduction

In the field of nuclear-physical research the cyclotron is an extremely useful apparatus, which has accordingly been adopted in various countries; a unit built by Philips is in use at the Institute for Nuclear-Physical Research at Amsterdam.

The cyclotron is an apparatus by means of which it is possible to impart to charged particles enormous speeds (corresponding to direct voltages of 10 million volts or more). One of the major components of the equipment is an electromagnet of very large proportions; 200 tons of iron were used in the construction of the magnet for the cyclotron under review, so that it was well worth while ascertaining beforehand the particular magnetic properties to which the metal should conform to give the best results. The outcome of these investigations is reviewed in this paper.

For a clearer understanding of the various questions involved, let us first call to mind some of the more general characteristics of ferromagnetic material, as this will enable us to classify the different materials according to their desired properties. Proceeding from considerations regarding the magnetic structure of ferromagnetic substances, we shall then be able to look into possible methods of influencing the properties of such materials. This will in turn explain the reasons for the choice of the particular kind of iron used in the construction of the cyclotron in question. A brief description will then be given of the method employed in the manufacture of this iron.

In the closing paragraph of this article it will be shown that the type of iron developed for the electromagnet of the cyclotron is also very suitable for the iron cores of relays as used in large numbers in automatic telephone exchanges.

The hysteresis curve with and without demagnetisation

The properties of ferromagnetic materials are known to be characterised by the relation between the magnetic induction, or flux density B — or the magnetisation J — and the magnetising field strength of force H. Let us consider J as a function or H, the relation between which is represented by a hysteresis curve. As the Giorgi system of units is employed in this article it is better, in plotting the curve, not to make use of H, but of $\mu_0 H$ (μ_0 is the permeability of a vacuum) for the abscissa. In the Giorgi system both $\mu_0 H$ and the magnetisation J are expressed in terms of Wb/m², and the abscissae and ordinates are then of the same denomination.

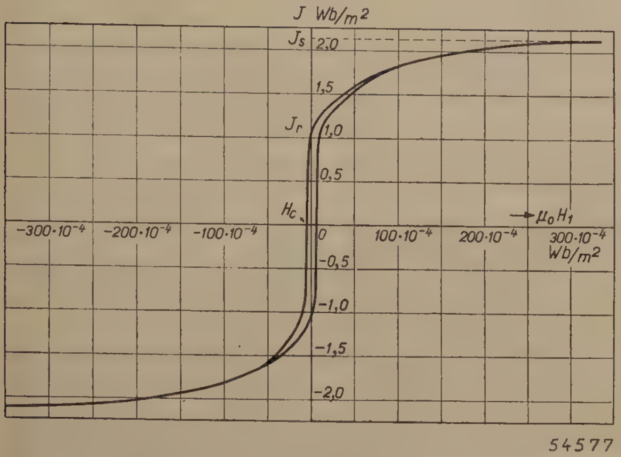

Fig. 1. Hysteresis curve of a ferromagnetic material. The curve relates to a closed magnetic circuit (e.g. an iron ring) and furnishes the relation between the magnetisation J and the field strength H_1 obtaining in the iron. At a high value of the field strength the magnetisation reaches a saturation point J_s. When it is subsequently reduced gradually to zero, J_s decreases to the remanence value J_r. Should an entire absence of magnetisation be desired, it is necessary to introduce a coercive force H_c the direction of which is opposed to that of the original magnetisation. The magnitude of the field strength H_1 is found by plotting $\mu_0 H_1$ (μ_0 being the permeability of a vacuum) in Wb/m² as abscissa; from this the field strength in oersted can be obtained by multiplying the resultant values by 10^4. The magnetisation J is similarly expressed in Wb/m². To obtain the corresponding values under the c.g.s. system the quantities must be multiplied by $10^4/4\pi \approx 800$.

When an ordinary hysteresis curve such as the one shown in *fig. 1* is examined, three important features are immediately apparent. At a high value of the magnetising force H the magnetisation attains a saturation value J_s; when the magnetising force is gradually reduced from this point to zero the magnetisation itself does not return to zero but goes no further than J_r, the remanence value, which is usually roughly equal to 0.5 J_s. Should an entire absence of magnetisation be desired, an external magnetic field H_c, the coercive force, must be applied in the opposite direction to that of the original field[1]).

Hysteresis curves, which are thus representative of one of the properties of a material, may be plotted from a closed magnetic circuit, e.g. a closed iron ring of uniform thickness, to which a magnetic field is applied. The field may be produced by a current flowing in a coil wound on the ring.

In an electromagnet we are not concerned with a closed circuit; in this case the circuit is interrupted by an opening known as the air-gap. It is important to know the relation between the magnetisation and the field strength H as determined by the coil in a circuit of this kind.

Even when the air-gap in the ring alluded to above is no wider than 0.25% of the total length of the iron, the form of the curve in fig. 1 undergoes a considerable change, as shown in *fig. 2* (curve *b*), representing the "shifted" curve.

A simple calculation will serve to reveal the nature of this change; it is actually brought about by the fact that in this case the field strength H_1 acting on the iron is no longer equal to the magnetic field strength H produced by the coil. The presence of the free end faces in the air-gap — which may be regarded as magnetic poles — sets up a demagnetising field in the iron.

To demonstrate this let us take the case of an iron ring (*fig. 3*), having in it a gap l_2 in width, the length of the iron as measured along the centre line being l_1 ($l_1 + l_2 = l$).

Suppose the air-gap to be so small that the spreading of the magnetic lines of force at the gap may be ignored; the magnetic flux density in the iron, B_1, will then be equal to that in the air, B_2. If we represent the (absolute) permeability by μ (μ_1 in iron; μ_2 in air), then $B_1 = B_2 = \mu_2 H_2$, where $\mu_2 = \mu_0 = 4\pi \cdot 10^{-7}$ H/m.

Now, assume that a current flowing in a coil wound round the ring produces an "external" magnetising force H; the

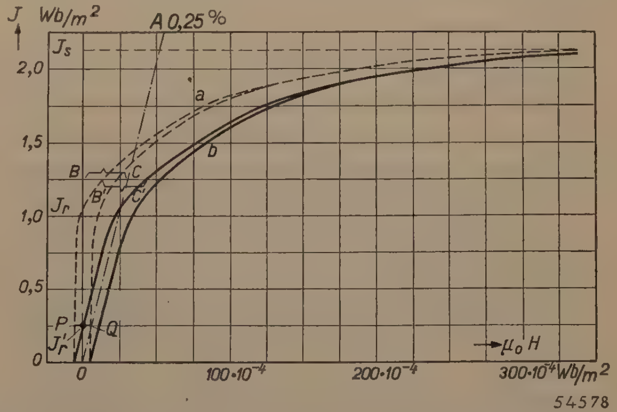

Fig. 2. The shifted hysteresis curve of an iron ring having in it an air gap the width of which is 0.25% of the total circumference. This curve illustrates the relation between the magnetisation and the "external" field strength H as determined by the current in the coil. The figure also shows how this shifted curve (*b*) may be derived from curve (*a*) (the "material" curve, fig. 1), by graphical transformation. Since, in order to obtain a certain magnetisation value J_1, the abscissa $\mu_0 H$ of a point on curve *a* must be augmented by NJ_1 (N being the demagnetisation factor), a line OA is drawn subtending an angle with the positive J-ordinate, the tangent of which is N. It is thus possible to read the value of NJ for every value of J (e.g. $B'C' = BC$). The quantity J_r in the case of curve *b* must be replaced by the apparent remanence J_r', which is considerably less. If, as the result of a low coercive force H_c, in conjunction with a high value of J_r, curve *a* is nearly enough perpendicular to the H-ordinate, then $J_r = \mu_0 H_c / N$. This will be apparent from the figure, provided $\overline{PJ_r'} = \overline{J_r' Q}$.

---

[1]) The coercive force is sometimes referred to as the strength of the field that must be applied to ensure a flux density of $B = 0$. In relation to the types of material discussed in this article (the coercive force of which is relatively low) this makes but little difference in practice.

latter is understood to be the force that would be set up by the coil without the iron. Taking the magnetising force within the iron to be H_1 and in the air-gap H_2, then:

$$Hl = H_1 l_1 + H_2 l_2 \quad \ldots\ldots\ldots \quad (1)$$

Making use of the fact that the flux density is equal to the magnetisation augmented by the flux density in vacuum, we then find (J_1 being the magnetisation of the iron) that:

$$B_1 = J_1 + \mu_0 H_1 \quad \ldots\ldots\ldots \quad (2)$$

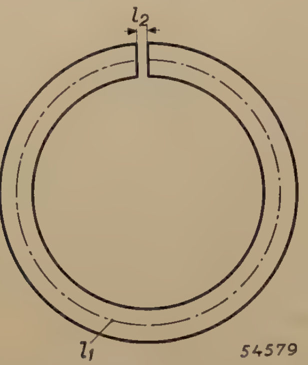

Fig. 3. Iron ring with air-gap l_2 in width; the length of the iron measured along the centre line is l_1.

In view of this, eq. (1) becomes:

$$Hl = H_1 l_1 + B_1 l_2/\mu_0 = H_1 l + J_1 l_2/\mu_0$$

or

$$\mu_0 H_1 = \mu_0 H - N J_1 \,, \quad \ldots\ldots\ldots\ldots \quad (3)$$

assuming that $l_2/l = N$.

It follows, then, that the magnetising force H_1 obtaining in the iron, owing to the presence of the air-gap, is smaller than the magnetizing force H as produced by the electric current. This fact may be so expressed that the iron is partially demagnetised by the opposing or demagnetising force NJ_1/μ_0.

The magnitude of the demagnetising force is determined by N, which in our example is the ratio between the width of the air-gap and the total length as measured along the centre line of the ring; in other words it is a magnitude depending wholly on the geometrical data of the magnetic circuit. N is actually known as the factor of demagnetisation.

Of the three quantities J_s, J_r, and H_c, J_s and H_c are not affected by this demagnetisation, but the remanence J_r changes to the apparent remanence J_r'. The order of size of the latter, as applied to fig. 1, depicting a hysteresis curve in which H_c is not too high, depends almost entirely on the values of H_c and N, but hardly at all on J_r, as will be readily appreciated.

Suppose the magnetisation curve of a closed ring has been plotted, for which purpose J is ascertained as a function of H, and it is desired to derive from it the shifted hysteresis curve relating to the case where an air-gap produces a demagnetisation effect as characterised by a factor N. Let us now see how this can be done by graphical transformation.

The measured hysteresis ("material") curve yields the magnetising force $H_1 = \mathrm{f}(J)$ within the iron. In a closed magnetic circuit the "external" magnetising force $H = H_1$, but according to eq. (3) $H_1 = H - NJ_1/\mu_0$ for a ring with air-gap. Thus, if we wish to know the relation between H and J we must make this distinction that without air-gap $H = \mathrm{f}(J)$ and with air-gap $H = \mathrm{f}(J) + NJ_1/\mu_0$, as illustrated by the shifted hysteresis curve. The latter can therefore be obtained from the original hysteresis curve by augmenting the abscissa $\mu_0 H_1$, for a given value J_1 of the magnetisation, by NJ_1. This is illustrated in fig. 2 for part of the curve in fig. 1. In order to determine graphically the quantity NJ_1, a line OA is drawn through the origin to subtend with the positive J-ordinate an angle the tangent of which is N.

If we are concerned with a material having only a low coercive force ($\mu_0 H_c = 0.1 \times 10^{-4}$ to 10×10^{-4}, i.e. 0.1 to 10 oersted), with normal $J_r = 0.5\ J_s$, the hysteresis loop at the point $\mu_0 H = -\mu_0 H_c$ is almost perpendicular to the H-ordinate and in this case the apparent remanence $J_r' = \mu_0 H_c/N$. This is immediately apparent when a line is drawn parallel to the H-ordinate through the point of intersection of the left-hand branch of the shifted hysteresis curve in fig. 2 and the J-ordinate (J_r'). Let the intersecting points of this line with the left-hand branch of the curve a and line OA be respectively P and Q; if the left-hand side of the curve a is practically perpendicular to the H-ordinate then PJ_r' and consequently also $\overline{QJ_r'} \approx \mu^{\circ} H_c$, from which it will at once be seen that $J_r' = \mu_0 H_c/N$.

In the situation shown in fig. 1, which concerns a fairly high coercive force ($\mu_0 H_c = 5 \times 10^{-4}$ Wb/m^2), the remanence is thus reduced to 0.20 of its original value at an air-gap width of 0.25%; were $\mu_0 H_c$ to be 0.5×10^{-4} Wb/m^2, J_r would even drop to 0.02 of that value.

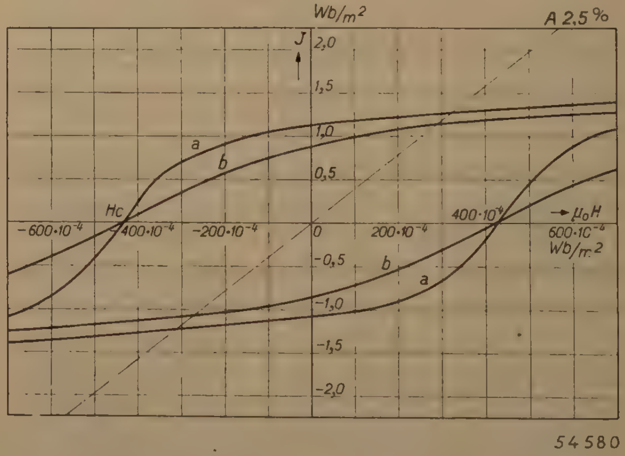

Fig. 4. Hysteresis curve for a material the coercive force of which is high. Curve *a* refers to the case where the demagnetisation (as in a closed iron ring) is zero, and curve *b* (the "displaced" hysteresis curve) to a ring with 2.5 % air-gap. It is seen that the apparent remanence in this case is governed mainly by the actual remanence and the factor of demagnetisation.

On the other hand, if the coercive force is quite high ($\mu_0 H_c = 100 \times 10^{-4}$ to 1000×10^{-4} Wb/m^2) as in *fig. 4*, then J_r' is only slightly less than J_r. For the above-mentioned air-gap of 0.25%, $J_r' = 0.985\ J_r$, whilst, for the demagnetisation illustrated in fig. 4 produced by a value of N which is 10 times higher, J_r' is still 0.80 J_r. In this case J_r' is thus determined mainly by the remanence and the factor of demagnetisation.

When it is considered, finally, that low values of H_c have narrow hysteresis loops, i.e. enclosing only a small area and consequently corresponding to low hysteresis losses, whereas high values of H_c give wide loops and high hysteresis losses, the following classification of ferro-magnetic materials according to their characteristics will be obvious as far as 1) and 2) are concerned; in 3) and 4) other properties are involved which often have to be taken into account as well.

Classification of ferro-magnetic materials and their applications

Distinction is made between materials with:

1) high H_c values ($\mu_0 H_c > 100 \times 10^{-4}$ Wb/m^2), i.e. magnetically "hard" materials,
2) low H_c value ($\mu_0 H_c < 10 \times 10^{-4}$ Wb/m^2) i.e. magnetically "soft" materials,
3) high magnetic saturation,
4) high electrical resistance, owing to which eddy current losses may be small.

When reviewing the applications of ferro-magnetic materials it will be found in every case that one or more of these characteristics are concerned, though possibly not just those which are desired.

In electro-magnets the aim is to produce the greatest possible magnetic flux in the iron with the least possible magnetising force. This means that the material should conform to category 3) above, but efforts will also be made to ensure that high saturation values at the lowest possible value of the magnetising force, in other words, a relatively very high remanence and not too wide a hysteresis loop, are obtained, as otherwise the return branch of the curve will yield high magnetisation at low field strength values, but not the ascending branch. The last mentioned requirement means that H_c must not be too high.

Permanent magnets, intended to produce intense magnetic fields within air-gaps, must be made from materials answering to requirement 1), for, notwithstanding the considerable demagnetisation by the air-gap, the apparent remanence must be high. Requirement 3) must, however, be satisfied as well, since high saturation is needed in order to ensure a high remanence J_r.

Materials employed for high-frequency work will, in the first place, be required to conform to requirement 4). "Ferroxcube", a type of material developed in recent years in the Philips Laboratories at Eindhoven, being non-metallic and having a high electrical resistance, is exceptionally suitable for the purpose, the more so since it also satisfies requirement 2), in that its hysteresis losses are very low.

In low-frequency technique requirements 2) and 4) are also important (e.g. in transformers), but 4) does not then carry so much weight, since a laminated construction easily reduces the eddy current losses to reasonable proportions, especially if iron alloys be used having a resistance several times higher than that of pure iron. It is an advantage, then, if the material satisfies requirement 3) as well, and this can be achieved by making use of the high saturation value of metallic iron, thus reducing to a great extent the physical dimensions of transformers.

In the case of relays, such as are used in large numbers in automatic telephone work, yet other requirements have to be specified: a relay is required to "close" on a certain relay current, that is, under a given "external" field. This might indicate requirements similar to those of other electro-magnets. What is more important, however, is that the relay should open when the relay current ceases to flow; in other words the remanence should be low. Generally speaking, this can be achieved by arranging for a small air-gap also in the "closed" position (e.g. by inserting a non-magnetic "anti-freezing" plate), so that the apparent and not the true remanence is involved. On the other hand, it is at least equally important for the coercive force to be as light as possible, and also that this value shall not increase in course of time; if the coercive force is not free of all tendencies to vary, even the best relay will stick in the end. This point is referred to again in the closing paragraph of this article.

Before going into the question of the manner in which the above requirements were fulfilled in practice in the manufacture of the iron for the electro-magnet of the cyclotron, let us try to form a clear mental picture of a ferro-magnetic material. Without entering too deeply into theoretical considerations regarding ferro-magnetism, it will be useful to mention one or two corollaries of the theory, limiting our review, however, mainly to those results which may explain the origin of a high remanence and low coercive force.

General conclusions to be drawn regarding a ferro-magnetic material

According to the usual conceptions, ferro-magnetic material in the unmagnetised state may be divided into a number of small elementary domains, called Weiss domains, the area of which is normally between 10 and 100 μ, the substance within these domains being fully saturated. When the condition of the material is such that it is wholly demagnetised or, at any rate, differs considerably from the condition of saturation J_s at the temperature considered, the magnetisation vectors of these zones are all differently oriented. The fact that the magnetisation in each elementary domain has a very definite direction means that from a magnetic aspect the different directions are not equivalent; in other words there apparently exist anisotropic magnetising forces which may be attributable to the following causes.

In the first place the magnetisation appears to follow certain preferential crystallographic directions, which may vary still further between different metals and alloys. In the case of pure iron the three mutually perpendicular, cubic, directions of the (body-centred) iron crystal may be said to provide preferential energy directions for the magnetisation, which means that the potential energy is lowest when the magnetisation is oriented in one of these preferential directions. The difference in the magnetic energy between the directions of easiest and most difficult magnetisation is sometimes referred to as the crystal energy E_k.

In the second place, preferential directions may occur as a result of internal strains, which are in turn connected with the phenomenon of magneto-striction. When a ferro-magnetic material is magnetised by an external field of increasing strength, those elementary domains which are favourably oriented with respect to this external field gradually grow at the expense of the less favourably oriented, so that the magnetisation vector comes to lie roughly in the direction of the field. At intense flux densities all these vectors ultimately assume that direction. The material thereby undergoes a change in form, dependent upon the variations in the direction of magnetisation, and reverts to normal when the field is removed. Conversely, elastic modifications of form must have an effect on the direction of magnetisation among the elementary domains. The magnitude of the preferential energy thus produced is determined by the product of the magnetostrictive constant λ (which is equal to the relative longitudinal variation between the fully demagnetised and saturated conditions of the material) and the amplitude of the fluctation in the internal strain σ_i.

Which of the above-mentioned anisotropic influences will tend to predominate depends on whether E_k is greater or less than $\lambda\sigma_i$. Even when E_k is very high as compared with $\lambda\sigma_i$, however, — and this is usually so in the case of iron — the anisotropic influence of the strains may still play an important part, since it is quite possible that, as a result of the magneto-striction, the preferential direction will almost coincide with one of the three crystallographic, preferential directions, thus involving a preference along this single axis instead of along three.

Thirdly, the form of the ferro-magnetic material has a direct bearing on the direction of magnetisation: this is related to the fact that the demagnetisation factor of such materials differs between one direction and another, and so also, therefore, does the strength of the demagnetising field. Even if we ignore the external shape of the material the "internal" form remains an important factor. This latter is governed by small non-magnetic inclusions 2) such as are present in all ferro-magnetic metals which are not absolutely pure. It would appear that, from the point of view of energy, it is much better for the magnetisation to run as far as possible parallel to such non-magnetic surfaces. This may be explaned by the fact that in the adverse case, independent magnetic poles will occur at the free surfaces, producing an opposed magnetic field.

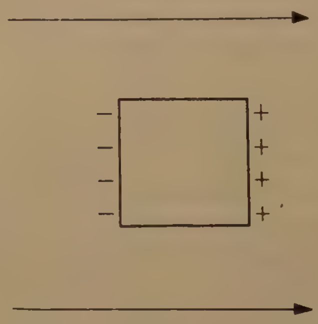

Fig. 5. How free magnetic poles occur in a cubic air-cavity. The arrows indicate the direction of magnetisation in the iron.

Let us suppose that a cubic air-cavity were to exist within an elementary domain (see *fig.* 5) and that this is required to produce no disturbance in the magnetisation around the cavity; in that case the magnetic flux density B_1 in the iron and that in the air, B_2, would have to be equal. This will occur provided no demagnetising poles are formed, i.e. when the magnetisation runs parallel to the air surface. If the non-magnetic inclusion be at all

---

2) When we speak here of non-magnetic inclusions we also mean those which, although magnetic, are less ferro-magnetic than the basic metal.

elongated in shape, magnetisation in the direction of the arrow (*fig. 6*) will be more favourable, from the aspect of the energy, than in the transverse direction.

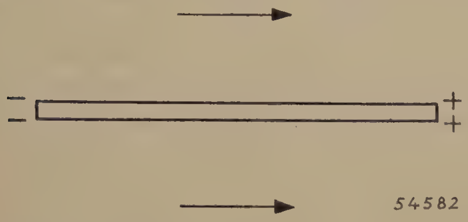

Fig. 6. How free magnetic poles occur if a non-magnetic inclusion has an elongated shape.

Moreover, non-magnetic inclusions tend to produce internal strains and thus also manifest themselves by their magneto-strictive effect.

Let us now see how the remanence and coercive force fit into the ferro-magnetic picture as sketched in the foregoing.

Remanence

The following simple considerations will serve to illustrate the relation between remanence and saturation.

Take the hypothetical case of a polycrystalline material in which so many anisotropic influences are at work that the preferential directions in the material as a whole are completely arbitrary. It might be expected of such a material in the fully demagnetised state ($J = 0$ and $H = 0$), such as might be produced by cooling the metal as from the Curie point in an external field of $H = 0$, that each elementary domain would have a certain optimum preferential direction, being the best from the point of view of energy, and that all the magnetisation vectors would thus be distributed at random over a sphere, in the manner illustrated in *fig. 7a*. If the metal be then saturated by means of a high magnetising force H in the direction indicated by the arrow in fig. 7, all the magnetisation vectors will assume this orientation (fig. 7*b*). When the field is removed the old preferential directions will be restored, but, since any two opposed directions are then equal as regards energy, the vectors will occupy only half the sphere (fig. 7*c*). This will gives us $J_r = J_s \overline{\cos \alpha}$, in which the vinculum over the "cos α" indicates that an average must be taken in respect of all angles occurring in this case over a hemisphere; this, then, yields $J_s = 0.5\ J_s$.

Now, it is possible to produce metals in which $J_r > 0.5\ J_s$, and we shall indicate the relevant requirements to be satisfied, together with the reasons for them. We shall suppose that fluctuations in the internal strain σ_i are so small that $\lambda\sigma_i \ll E_k$ and, further, that non-magnetic inclusions are either entirely absent or so large in proportion as to be magnetically innocuous (their dimensions being of the same order as the elementary domains). We then have to reckon only with the anisotropic crystallographic structure; the magnetisation vectors in all the elementary domains will then be oriented in one of the crystallographic preferential directions. After saturation in accordance with fig. 7*b*, the remanence of iron will not be as shown in fig. 7*c*, but as in fig. 7*d*, since the cubic axis most closely approximating the direction of the field will be the preferential direction taken. The half-angle of the sector of a sphere, thus occupied, is about 58°, this being the angle between a body diagonal and one edge of a cube. It is clear that this half-angle cannot be greater than 58°, for this will in any case include at least one of the axes of the cube functioning as preferential direction. In this case the remanence is found from the mean of $J_s \cos \alpha$, not with respect to the hemisphere (90°), but over a sector of the sphere the half angle of which is 58°, so that:

$$J_r = 0.78\ J_s.$$

The above argument thus provides the requirements to be satisfied by the iron to ensure a high remanence value, viz. the internal strains must not be great and non-magnetic inclusions

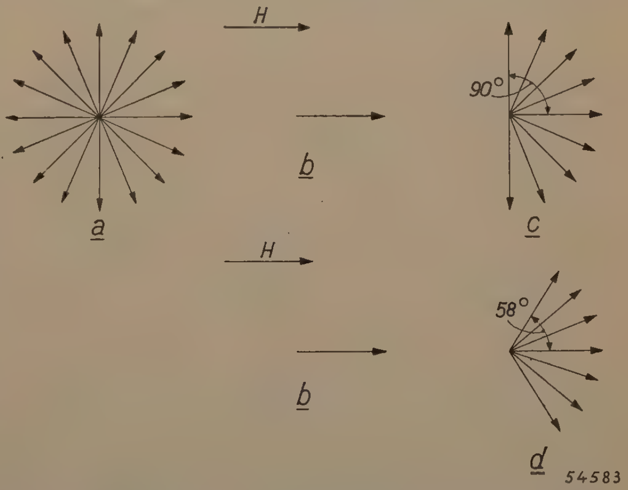

Fig. 7. Diagrammatic representation of the direction of the magnetisation vectors of the elementary domains of a polycristalline, ferromagnetic material.

a) in the fully demagnetised state the directions of the vectors are arbitrarily distributed;

b) when the material is saturated by means of an external magnetising force H, all the vectors assume the direction of H;

c) after the external magnetising force is removed, the vectors will be distributed over half a sphere;

d) when $\lambda\sigma_i \ll E_k$ (where E_k relates to a cubic structure) and the non-magnetic inclusions are absent or have very little influence, the vectors are contained within a sector of a sphere having a half-angle of 58°.

must be as few as possible. The same conditions, albeit for a different reason, also ensure a low coercive force.

The coercive force

In order to demonstrate the relation between strains and inclusions on the one hand and the coercive force on the other, it would be necessary to penetrate rather more deeply into the theory of the coercive force than can be done in this paper. A few words will, however, be said on the subject.

As already pointed out, the "magnets" in the elementary domains are parallel to each other, so that each domain is always saturated, at any rate as far as the temperature movement permits. At the boundary between two such domains a transition occurs between the preferential direction of one domain and the other, and in this transitional area, which may be referred to as the "wall" of the elementary domain,

1) the magnets are no longer parallel to each other, which means a loss of energy, and
2) they assume a direction of magnetisation which need not necessarily be the same as the local preferential direction, this likewise involving loss of energy.

The "wall" thus possesses a certain amount of energy per cm^2 of its area.

Now, it appears that the macroscopic magnetisation of magnetically soft metals takes place at relatively low values of the coercive force, by reason of a displacement of these walls, in consequence of which the domains which are more easily magnetised with respect to the external field increase in size, whilst the less favourably oriented domains are "absorbed". The magnitude of the coercive force of the material is determined by the facility (at low H_c) or the difficulty (at higher H_c) with which the walls can be displaced.

What, then, are the obstacles to these displacements of the walls? In the first place it may be imagined that the energy of the wall itself is a function of the locality where the wall occurs, either by reason of the fact that the energy per cm^2 varies owing to fluctations in the strain (σ_i), or because there may be non-magnetic inclusions in the wall which reduce the total wall area to be taken into account. In these wall displacements small amounts of energy have to be constantly added, disappearing again in the form of heat. Both the fluctuations in strain and the non-magnetic inclusions thus tend to increase the coercive force.

Finally, it should be noted that within the elementary domains themselves internal strains set up minor variations in the direction of the magnetisation, whilst inclusions produce small fluctuations in the intensity of the magnetisation, both these effects resulting in a loss of magnetising energy.

It has been stated above that non-magnetic inclusions represent demagnetising energy. Without going into quantitative calculations, from the diagrams *a* and *b* in *fig. 8* it will be readily seen that the demagnetising energy in case *b* is much greater than in case *a*. When the wall shown in fig. 8*a* is moved so that the inclusion lies well within a single elementary domain, there is not only the increase in energy due to the increase in the wall area but also an increase due to this augmented demagnetisation energy. The shape and dimensions of the inclusion determine which of the two effects predominates. The fluctuations in the direction of magnetisation in the body of an elementary zone, alluded to above, also give rise to hypothetical magnetic charges and thus also to variations in energy when the location of the wall is changed. In this way, depending on the location of the wall, fluctuations in energy may have the effect of increasing the coercive force.

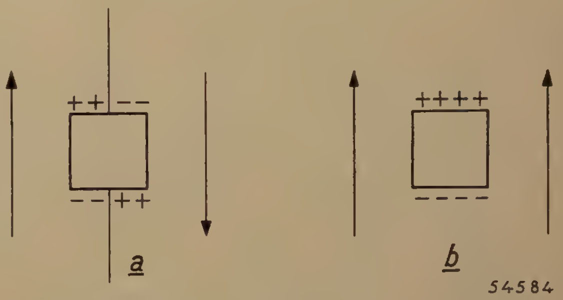

Fig. 8. Effects of the "wall" of an elementary domain on the magnitude of the demagnetising energy arising from non-magnetic inclusions.
a) A cubic inclusion at the boundary between two elementary domains.
b) The inclusion within a single elementary domain. In the second instance the demagnetising energy is much greater than in the first.

The conclusion to be drawn is that the conditions to be met by the iron to ensure a low coercive force are: low internal strains and as few non-magnetic inclusions as possible, i.e. the same as for a high remanence.

Iron for the electromagnet of a cyclotron

In the light of the foregoing considerations it is clear that the ferromagnetic material employed in the construction of electromagnets should satisfy the requirements mentioned above as regards internal strains and non-magnetic or only weakly magnetic inclusions. Furthermore, we must ensure high saturation J_s in order to obtain a high remanence in an absolute sense.

Starting out from the latter requirement, it is important to note that the magnetic saturation value of pure iron is already quite high, namely 21 000 × 10^{-4} Wb/m² (approx. 1700 c.g.s. units). Still higher values can be obtained only by the addition of large proportions (15 to 35%) of cobalt, which is very costly; the J_s value then rises slightly, viz. to 2.25-2.50 Wb/m². Any other element that is soluble in iron will reduce the saturation point. It might be asked: Why not then use an iron that is pure and free from strain? But it is not possible to produce such iron on a technical scale, so that we have to ascertain how, and in how far, the detrimental elements in the iron can be eliminated.

In the list of ever-present constituents of iron which are highly detrimental from the aspect of magnetisation of the soft metal, carbon is the outstanding element. Carbon, which is practically insoluble in iron at ambient temperatures, usually occurs in the form of cementite (Fe_3C), which is meta-stable at these temperatures, the more stable form at such temperatures, namely graphite, being much more difficult to produce. Despite the fact that cementite is in itself still slightly magnetic, it has a much more adverse effect, appearing as it does as inclusions, than non-magnetic graphite, if only for the reason that a given percentage of carbon produces a much greater volume of cementite than graphite, viz. 4.5 times as much. A content of 6.7% carbon by weight is sufficient to convert the whole of the iron into cementite.

The simplest means of removing the carbon from the iron consists in burning it out with oxygen, to form CO, and this can be done during the smelting process, either by forcing air through the metal or by adding sufficient quantities of iron oxide, for instance in the form of ore. The latter method is employed by the firm of De Muinck Keyzer of Utrecht, the suppliers of the iron used for the electromagnet of the cyclotron at Amsterdam. This oxidation process was carried out in a Siemens-Martin furnace, in which the iron was melted under a layer of molten slag, just so long until the carbon content dropped below 0.06%. The metal ultimately contained an excess of oxygen, which was then removed immediately before casting by adding so much aluminium that about 0.5% Al is left in the melt; this had the effect of fixing the oxygen in the form of Al_2O_3, an important part of which finished up in the slag. In addition to the 0.5% Al, 0.5% Si was added, in view of the fact that any carbon still present in the iron should preferably take the form of graphite. Although, in contrast with cementite, graphite is the stable modification at low temperatures, it is so difficult to produce that, unless special precautions be taken to ensure its formation, very little of it appears at all. Now, both silicon and aluminium possess the property of being able to promote the formation of graphite. These two elements were added to the melt as a mixture, because it was felt that the graphite-forming properties would be more pronounced in the combined than in the separate elements.

The addition of Al and Si naturally has the drawback that they both tend to reduce the saturation induction of the iron; the J_s value of the iron produced in the above manner is about 2.0 Wb/m² and the chemical composition is roughly as follows:

Fe	98.9 %
C	0.05%
Si	0.45%
Al	0.35%
Mn	0.25%.

This reveals the fact that part of the aluminium used for the de-oxidation disappeared in the slag; manganese is a comparatively innocuous element occurring in all technical grades of iron.

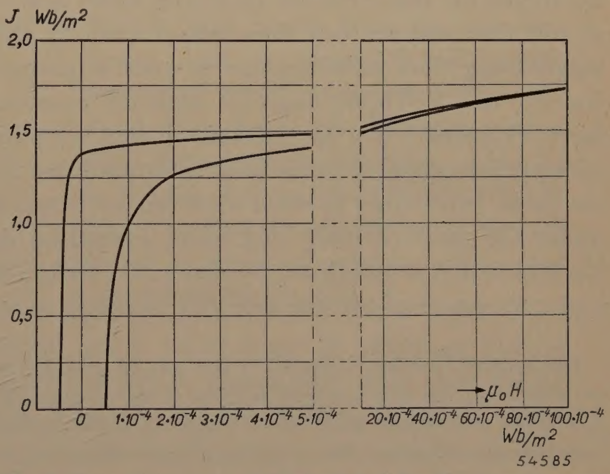

Fig. 9. Hysteresis curve of the iron used for the electromagnet of a cyclotron. The saturation induction J_s is 2.0 Wb/m², but this is attained at so high a field strength that it cannot be read from the graph. The remanence is approximately 70% of J_s, and the coercive force is very low (u_0H_c = 0.5 × 10^{-4} Wb/m²). For $\mu_0H_c > 5 \times 10^{-4}$ a different scale is used from that in respect of $\mu_0H_c < 5 \times 10^{-4}$.

Fig. 9 illustrates the hysteresis curve of a casting made from the iron in question: the remanence is about 70% of the saturation of 2.0 Wb/m² and the latter is reached at so high a field strength that it can no longer be read from the graph. This, then, is an example of a metal in respect of which $J_r >$ 0.5 J_s. For a technical grade of iron the coercive force is very low, viz. $\mu_0 H_c = 0.5 \cdot 10^{-4}$ Wb/m², this being an average. Needless to say, different casts yield varying values, but the coercive force is in every case so low that it lies between 0.3×10^{-4} and 0.7×10^{-4} Wb/m².

Table I. Comparative magnetic properties of different kinds of soft iron.

Grade of iron	Magnetising force (in $\mu_0 H$) to give $J = 1.5$ [3]) [4]) Wb/m².	Coercive force ($\mu_0 H_c$ in Wb/m²).
Mild steel	20×10^{-4}	$(1.5\text{-}3) \times 10^{-4}$ *)
Hyperm 0 (free-cutting quality)	23×10^{-4}	$(0.8\text{-}1,5) \times 10^{-4}$
Dynamo iron	16×10^{-4}	1×10^{-4}
Hyperm 0 (standard)	12.5×10^{-4}	$(0.5\text{-}1) \times 10^{-4}$
Armco iron	10×10^{-4}	1×10^{-4} *)
Cyclotron iron	8×10^{-4}	$(0.3\text{-}0.7) \times 10^{-4}$
Wemco iron (99.95 Fe)	1×10^{-4}	0.05×10^{-4}

*) The metals are subject to variation on ageing (H_c increases).

[3]) Corresponding to 1200 c.g.s. units or 15 000 gauss.

[4]) To obtain the flux density in oersted, multiply these values by 10^4.

To what extent the characteristics of the iron developed for the cyclotron excel over other grades of soft iron will be seen from *table I* showing the magnetising force to be applied to yield a magnetisation of 1.5 Wb/m², together with the coercive force. Hyperm 0 is a special kind of iron used by Krupp for relays. Wemco iron, mentioned last in the table, is included to show what can be attained under the most carefully controlled conditions in the laboratory, although not of course on a technical scale; no practical use can therefore be made of it.

The magnetic properties desired in soft iron for a cyclotron are related to the field strength required in the air gap. The desiderata and values given above apply to the cyclotron built for the Institute for Nuclear-Physical Research at Amsterdam. If, for a cyclotron of the same capacity, the dimensions of the pole shoes should have to be reduced, higher field strengths would be needed and the saturation value J_s of the soft iron would have to be raised, necessitating a different choice of the composition of the material.

Iron as used for relays

It has already been pointed out that iron used for the cores of relays must show the lowest possible values of the coercive force. Further we have shown that the properties of iron intended for the electromagnet of a cyclotron (low internal strain and absence of non-magnetic inclusions) ensure a low coercive force. The obvious inference is that the same iron which is suitable for the cyclotron will also be a very satisfactory material for the manufacture of relays.

In passing, we stated above that the coercive force of the iron used for relays must not increase as a result of ageing. The coercive force must be low in order to ensure a low apparent remanence. This is important, as it makes it possible for the relays to be so adjusted as to prevent sticking. If the coercive force does increase with the age of the relay the apparent remanence may even become so high that the relay will fail to open altogether. Many ordinary technical grades of iron do possess this disadvantage. The causes of this phenomenon may be sought in a precipitation process in which especially nitrogen and, to a certain extent, also carbon are the harmful elements, since they tend to separate in the form of nitrodes and carbides. Nitrogen is almost wholly insoluble in iron at ambient temperatures and only slightly soluble at elevated temperatures, but the γ-phase of iron, which is stable between 900 and 1400 °C, has a great solubility for nitrogen. However, when iron containing nitrogen is cooled down this element does not immediately pass out of solution as a nitride; in other words, the solution is super-saturated and if nitrides are formed in the course of time they occur in the iron in a very finely divided form, disturbing the crystal lattice and producing internal strains and non-magnetic inclusions, both of which increase the coercive force. To counteract this effect, silicon and aluminium should also be added to the iron, not only because they fix and remove the nitrogen as well as the oxygen, but also because they reduce the temperature range within which the iron is in the face-centred and not in the body-centred phase. Such percentages of these elements as are mentioned in a preceding section will reduce the range in question from 900-1400 °C to 1000-1300 °C; the smaller this range can be made and the higher the transition temperature between the body-centred and face-centred phases, the smaller the content of nitrogen that will remain in the super-saturated solution. The type of iron under review, to which small quantities of Si and Al are added, is perfectly free from any tendency towards ageing; heating of the metal for 500 hours at 100 °C has not the slightest effect on the coercive force.

ABSTRACTS OF RECENT SCIENTIFIC PUBLICATIONS OF THE N.V. PHILIPS' GLOEILAMPENFABRIEKEN

Reprints of these papers not marked with an asterisk can be obtained free of charge upon application to the Administration of the Research Laboratory, Kastanjelaan, Eindhoven, Netherlands.

1719b: E. J. W. Verwey and J. Th. G. Overbeek: Long distance forces acting between colloidal particles (Trans. Faraday Soc. **42B**, 117-123, 1946).

The writers have made an extensive investigation on the theory of the long distance forces acting between the particles in a colloidal solution, more especially in the case where the particles are surrounded by an electrical double layer. The paper gives a brief summary of these investigations preceded by a critical discussion of the work of previous authors.

For more extensive information, see these abstracts, Nr. **1769**.*

1764: E. J. W. Verwey: De vrije energie van phasengrenzen (Kon. Vl. Acad. Wet. Lett. Sch. Kunsten; symposium Grenslaagverschijnselen, gehouden te Brussel, 5 en 6 Juli 1946, blz. 20-37, 1947). (The free energy of phase boundaries, in Dutch).

The free energy of a phase boundary has been considered for a number of simple cases. It is shown that in the cube face of most alkalihalides the negative ions are shifted outward, the positive ions inward. The deformations have the effect of lowering the free surface energy. The surface energy of water can roughly be understood by considering its ice-like structure and the forces acting between the molecules. The effects of dissolved substances on the surface tension of liquids is discussed qualitatively and the considerations are extended to the case of an interface of two liquids where an electric double layer may be present.

1764a: J. Th. G. Overbeek: Wisselwerking van electrochemische dubbellagen. Stabiliteit van hydrophobe colloiden (Kon. Vl. Acad. Wet. Lett. Sch. Kunsten; symposium Grenslaagverschijnselen, gehouden te Brussel, 5 en 6 Juli 1946, blz. 130-156, 1947). (Interaction of electrochemical double layers. Stability of hydrophobic colloids; in Dutch).

Considerations on the structure of the electrochemical double layer lead to a relation between the charge and the potential of a surface in contact with a solution of an electrolyte. It is shown that the surface charge will be diminished by the interaction of two double layers, causing a repulsion. Apart from this repulsion the London-van der Waals attraction has to be taken into account. Attraction and repulsion are given in the form of potential curves. If the combined potential curve shows a maximum of sufficient height, the corresponding sol is stable. Important conclusions are: a proof of the validity of Schulze and Hardy's rule for the concentration of electrolyte necessary to flocculate a hydrophobic sol, an estimate of the London-van der Waals constant, a proof of the instability of a solution with very small colloidal particles ($< 10^{-7}$ cm). Slow flocculation of a hydrophybic sol is a selfretarding process. The stability of coarse suspensions demonstrate that the London-van der Waals forces must decay more rapidly than according to customary theory, owing to a retardation effect. The reader is further referred to these abstracts, No. **1769***.

1764b*: W. Ch. van Geel: Doorgang van electronen door grenslagen (sperlaaggelijkrichters en sperlaagfotocellen) (Kon. Vl. Acad. Wet. Lett. Sch. Kunsten; symposium Grenslaagverschijnselen, gehouden te Brussel, 5 en 6 Juli 1946, blz. 172-192, 1947). (Passage of electrons through barrier layers; barrier-layer-rectifiers and -photocells; in Dutch).

In this paper the passage of electrons through insulating layers is considered. This phenomenon chiefly depends on the nature of the adjacent electrodes. Barrier layers, *a*) between two metals, *b*) between a metal and a semi-conductor, *c*) between a metal and an electrolyte and *d*) between a metal and a semi-conductive photosensitive substance are dealt with in succession. Various theories, based on tunnel-effect, cold emission and double layers are shortly described and compared with experimental results.

1783/85: H. Rinia, J. de Gier and P. M. van Alphen: Home projection television, I. Cathode ray tube and optical system; G. J. Siezen and F. Kerkhof: Id. II. Pulse-type high-voltage supply;

J. Haantjes and F. Kerkhof: Id. III. Deflection circuits (Proc. Inst. Radio Engr. **36**, 395-411, 1948, No. 3).

The contents of these papers are more extensively dealt with in Philips techn. Rev. **10**, 1948/49, Nos 3, 4, 5, 10 and 12, under the title: "Projection television receiver".

1786: H. C. Hamaker: Een systematische vergelijking van de statistische eigenschappen van hedendaagse steekproef-schema's (Statistica **2**, 19-39, 1948, No. 1/2). (A systematic comparison of the statistical properties of present-day sampling-schemes; in Dutch).

A survey of various sampling schemes, carried out with the aid of the "random walk diagram", leads to the conception that it must be possible to effect the same degree of inspection by the application of different schemes. The degree of inspection of a scheme is contained in its "operating characteristic", which is specified by two constants viz: its centre q_0, for which $P = {}^1/_2$, and its slope s in this point, defined by $s = -(\mathrm{d}P/\mathrm{d}q)_{q=q_0}$, q being the quality of the batch and P the chance of it not being rejected. It is shown that, if the operating characteristics of two different sampling schemes possess the same values of q_0 and s, the two characteristics are almost completely coincident. Thus two sampling schemes having the same q_0 and s will give identical inspection performances, and are consequently defined as "equivalent". A comparison of the sample sizes of equivalent schemes leads to a general definition of the "efficiency" of a scheme. On this basis single, double and sequential schemes are intercompared.

1787: J. L. Snoek: Dispersion and absorption in magnetic ferrites at frequencies above one Mc/s (Physica **14**, 207-217, 1948, No. 4).

The phenomena of absorption and dispersion observed in magnetic ferrites at frequencies above one Mc/s are discussed making the assumption that at these frequencies no contribution to the magnetisation is made by the Bloch boundaries.

For pure and unstrained polycrystalline aggregates of cubic crystals the following relation between the critical frequency and the initial susceptibility is found to be equal to ${}^2/_3\ |g|\ M$ where $g = e/mc = 1{,}76 \cdot 10^7$ emu and M the magnetic moment per cm^3. In deriving this equation the damping is assumed to be small. It is further shown that internal stresses tend to increase the losses at lower frequencies and make the rise in tan δ with frequency less steep. This is actually borne out by experiment.

1788: W. Opechowski: On the anisotropic exchange interaction and the behaviour of copper potassium sulphate at very low temperatures (Physica **14**, 237-248, 1948, No. 4).

Formulae are given for the specific heat and the magnetic susceptibility of a crystal, calculated on the assumption that the interaction between magnetic atoms is a sum of the anisotropic (direct or indirect) exchange interaction and the magnetic interaction. These formulae are applied to the case of copper potassium sulphate which has been investigated experimentally by De Klerk at temperatures below 1° K. Unfortunately, no unambiguous theoretical conclusions seem to be possible.

1789: H. Brinkman: Réflexion résultante par plusieurs couches parallèles (Revue d'optique **27**, 31-33, 1948, No. 1). (Resulting reflection by a number of parallel layers; in French).

A simple deduction is given of T. Smith's formula for the reflection of a system of (m—1) parallel non absorbing layers. This formula expresses that the ratio between the resulting reflectivity and the resulting transmission equals the sum of the corresponding ratios for the separate layers, taking into account repeated reflexions and considering the different rays as incoherent (thick specimen or white light). The resulting reflexion is minimal if the refractive index of each layer is equal to the geometric mean of the indices of adjacent layers. In good approximation it may be said that for given initial and final mediums the reflexion then is $1/m$ of the reflexion existing in the case of one optical surface.